

# Mitigating realistic noise in practical noisy intermediate-scale quantum devices

Jinzhao Sun,<sup>1,\*</sup> Xiao Yuan,<sup>2,3,†</sup> Takahiro Tsunoda,<sup>1</sup> Vlatko Vedral,<sup>1,4</sup> Simon C. Benjamin,<sup>2</sup> and Suguru Endo<sup>2,5,‡</sup>

<sup>1</sup>Clarendon Laboratory, University of Oxford, Parks Road, Oxford OX1 3PU, United Kingdom

<sup>2</sup>Department of Materials, University of Oxford, Parks Road, Oxford OX1 3PH, United Kingdom

<sup>3</sup>Stanford Institute for Theoretical Physics, Stanford University, Stanford California 94305, USA

<sup>4</sup>Centre for Quantum Technologies, National University of Singapore, Singapore 117543, Singapore

<sup>5</sup>NTT Secure Platform Laboratories, NTT Corporation, Musashino 180-8585, Japan

(Dated: June 20, 2022)

Quantum error mitigation (QEM) is vital for noisy intermediate-scale quantum (NISQ) devices. While most conventional QEM schemes assume discrete gate-based circuits with noise appearing either before or after each gate, the assumptions are inappropriate for describing realistic noise that may have strong gate-dependence and complicated nonlocal effects, and general computing models such as analog quantum simulators. To address these challenges, we first extend the scenario, where each computation process, being either digital or analog, is described by a continuous time evolution. For noise from imperfections of the engineered Hamiltonian or additional noise operators, we show it can be effectively suppressed by a novel stochastic QEM method. Since our method only assumes accurate single qubit controls, it is applicable to all digital quantum computers and various analog simulators. Meanwhile, errors in the mitigation procedure can be suppressed by leveraging the Richardson extrapolation method. As we numerically test our method with various Hamiltonians under energy relaxation and dephasing noise and digital quantum circuits with additional two-qubit crosstalk, we show an improvement of simulation accuracy by two orders. We assess the resource cost of our scheme and conclude the feasibility of accurate quantum computing with NISQ devices.

With the experimental demonstration of quantum supremacy [1], whether current or near-future noisy intermediate-scale quantum (NISQ) devices are sufficient for realising quantum advantages in practical problems becomes one of the most exciting challenges in quantum computing [2]. Since NISQ devices have insufficient qubits to implement fault-tolerance, effective quantum error mitigation (QEM) schemes are crucial for suppressing errors to guarantee the calculation accuracy to surpass the classical limit. Among different QEM schemes via different post-processing mechanisms [3–27], the probabilistic QEM method is one of the most effective techniques [4, 5], which fully inverts noise effect by requiring a full tomography of the noise process and assuming noise independently appears either before or after each gate in a digital gate-based quantum computer. While these assumptions are adopted for many QEM schemes, realistic noise is more complicated. Specifically, since every gate is experimentally realised via the time evolution of quantum controls [1, 28–36], noise happens along with the evolution, whose effect inevitably mixes with the gate or process and even scramble nonlocally [37]. For example, as one of the major noise in superconducting qubits, crosstalk of multi-qubit gates originates from the imperfect time evolution with unwanted interactions [29–31, 36, 38, 39]. Therefore, such inherent dynamics-based and nonlocal noise effects make conventional QEM schemes less effective for practical NISQ devices. Meanwhile, a more natural and noise-robust computation model is via analog quantum simulators [40–57], which directly emulate the target system without even implementing gates. It also remains an important open challenge to suppress errors for reliable medium- or

large-scale analog quantum simulators [58, 59].

In this work, we present QEM schemes without assumptions of gate-based circuits or simplified local noise models of each gate. Specifically, we introduce *stochastic error mitigation* for a continuous evolution with noise described by imperfections of the engineered Hamiltonian or super-operators induced from the interaction with the environment [47, 59–61]. Compared to existing methods, such as dynamical decoupling, which are generally limited to low frequency noise and small simulations [62–65], our work introduces a universal way to mitigate realistic noise under experiment-friendly assumptions. Our work considers continuous evolution of the system and assumes accurate single-qubit operations, which is applicable to all digital quantum simulators and various analog simulators. Our method is compatible with existing QEMs, and its combination with Richardson extrapolation can be further leveraged to suppress errors in inaccurate model estimations and recovery operations. We numerically test our scheme for various Hamiltonians with energy relaxation and dephasing noise and a quantum circuit with two-qubit crosstalk noise. We conduct a resource estimation for near-term devices involving up to 100 qubits and show the feasibility of our QEM scheme in the NISQ regime.

**Framework.**— We first introduce the model that describes either gate syntheses or continuous processes in digital or analog simulation. We consider the ideal evolution of state  $\rho_I(t)$  with a target Hamiltonian  $H_{\text{sys}}$  as

$$\frac{d\rho_I(t)}{dt} = -i[H_{\text{sys}}(t), \rho_I(t)]. \quad (1)$$

In practice, we map  $H_{\text{sys}}$  to a noisy controllable quantum

hardware  $H_{\text{sim}}$ , whose time evolution is described by the Lindblad master equation

$$\frac{d\rho_N(t)}{dt} = -i[H_{\text{sim}}(t), \rho_N(t)] + \lambda \mathcal{L}_{\text{exp}}[\rho_N(t)], \quad (2)$$

where  $\rho_N(t)$  is the noisy state,  $\mathcal{L}_{\text{exp}}$  is the noise super-operator with error strength  $\lambda$  [47, 59], and  $H_{\text{sim}} \neq H_{\text{sys}}$  corresponds to coherent noise. Suppose we are interested in measuring the state at time  $T$  with an observable  $O$ . The task of QEM is to recover the noiseless measurement outcome  $\langle O \rangle_I = \text{Tr}[O\rho_I(t)]$  via noisy process.

In general, it would be difficult to efficiently mitigate arbitrary noise with any noise strength. Here, we assume that the noise operators act weakly, locally and time-independently on small subsystems. Even though, local noise operators at instant time  $t$  can easily propagate to become global noise after integrating time [37]. We also assume that accurate individual single-qubit controls are allowed, which holds for digital NISQ devices where single-qubit operations can achieve averaged fidelity of 99.9999% [66] whereas the record for two-qubit fidelity is three orders lower [67, 68]. While not all analog quantum simulators support individual single qubit controls, they can indeed be achieved in various platforms with superconducting qubits [29, 69–72], ion trap systems [51, 73, 74], and Rydberg atoms [75]. Therefore, our framework is compatible with various practical NISQ devices. In the following, we focus on qubit systems and assume time-independent noise. We note that the discussion can be naturally generalised to multi-level systems, as well as general time-dependent noise [37].

*Continuous QEM.*— We first introduce ‘continuous’ QEM as a preliminary scheme as shown in Fig. 1(a). Consider a small time step  $\delta t$ , the discretised evolution of Eqs. (1) and (2) can be represented as

$$\rho_\alpha(t + \delta t) = \mathcal{E}_\alpha(t)\rho_\alpha(t). \quad (3)$$

Here  $\alpha = I, N$  and  $\mathcal{E}_\alpha(t)$  denotes the ideal ( $\alpha = I$ ) or noisy ( $\alpha = N$ ) channel that evolves the state from  $t$  to  $t + \delta t$  within small  $\delta t$ . We can find a recovery operation  $\mathcal{E}_Q$  that approximately maps the noisy evolution back to the noiseless one as  $\mathcal{E}_I(t) = \mathcal{E}_Q\mathcal{E}_N(t) + \mathcal{O}(\delta t^2)$ . The operation  $\mathcal{E}_Q$  is in general not completely positive, hence cannot be physically realised by a quantum channel. Nevertheless, similar to probabilistic QEM for discrete gates [4, 5], we can efficiently decompose  $\mathcal{E}_Q$  as a linear sum of a polynomial number of physical operators  $\{\mathcal{B}_j\}$  that are tensor products of qubit operators,

$$\mathcal{E}_Q = c \sum_j \alpha_j p_j \mathcal{B}_j, \quad (4)$$

with coefficients  $c = 1 + \mathcal{O}(\delta t)$ ,  $\alpha_j = \pm 1$ , and a normalised probability distribution  $p_j$ . We refer to [37] for details of the decomposition and its optimisation via linear programming. Under this decomposition, the whole

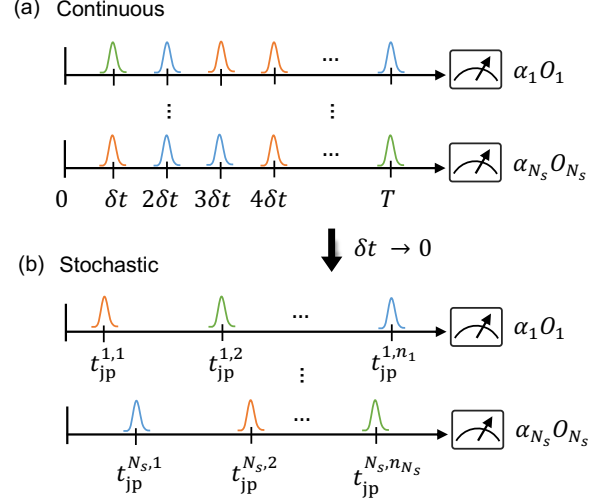


FIG. 1. (a) Continuous QEM. With discretised time step  $\delta t$ , each recovery operation is weakly and ‘continuously’ acted after each noisy evolution of time  $\delta t$ . Here different color represents different recovery operations. The output state is measured and repeated to obtain  $N_s$  outcomes  $\{O_m\}$ , and their average corresponds to the error mitigated outcome. (b) Stochastic QEM. We can equivalently realise (a) by  $\delta t \rightarrow 0^+$  and randomly applying a small number  $n_m$  of strong recovery operations as in Algorithm 1. The time  $\{t_{jp}^{m,k}\}_m$  to apply recovery operations of the  $m$ th run are predetermined, which can be further pre-engineered into the original evolution via a noisy time evolution of a modified Hamiltonian.

ideal evolution from 0 to  $T$  can be mathematically decomposed as

$$\prod_{k=0}^{n-1} \mathcal{E}_I(k\delta t) = C \sum_{\vec{j}} \alpha_{\vec{j}} p_{\vec{j}} \prod_{k=0}^{n-1} \mathcal{B}_{j_k} \mathcal{E}_N(k\delta t) + \mathcal{O}(T\delta t), \quad (5)$$

where  $n = T/\delta t$ ,  $C = c^n$ ,  $\alpha_{\vec{j}} = \prod_{k=0}^{n-1} \alpha_{j_k}$ ,  $p_{\vec{j}} = \prod_{k=0}^{n-1} p_{j_k}$ , and  $\vec{j} = (j_1, \dots, j_{n-1})$ . Denote the ideally evolved state as  $\rho_I(T) = \prod_{k=0}^{n-1} \mathcal{E}_I(k\delta t)\rho(0)$  and the noisily evolved and corrected state as  $\rho_{Q,\vec{j}}(T) = \prod_{k=0}^{n-1} \mathcal{B}_{j_k} \mathcal{E}_N(k\delta t)\rho(0)$ , we can approximate the ideal state  $\rho_I(T)$  as a linear sum of noisy states as  $\rho_I(T) = C \sum_{\vec{j}} \alpha_{\vec{j}} p_{\vec{j}} \rho_{Q,\vec{j}}(T) + \mathcal{O}(T\delta t)$ . When measuring an observable  $O$  of the ideal state, the ideal measurement outcome  $\langle O \rangle_I = \text{Tr}[\rho_I(T)O]$  is also approximated as a linear sum of the noisy measurement outcomes  $\langle O \rangle_{Q,\vec{j}} = \text{Tr}[\rho_{Q,\vec{j}}(T)O]$  as

$$\langle O \rangle_I = C \sum_{\vec{j}} \alpha_{\vec{j}} p_{\vec{j}} \langle O \rangle_{Q,\vec{j}} + \mathcal{O}(T\delta t). \quad (6)$$

In practice, we can randomly prepare  $\rho_{Q,\vec{j}}(T)$  with probability  $p_{\vec{j}}$ , measure the observable  $O$ , and multiply the outcome with the coefficient  $C\alpha_{\vec{j}}$ . Then the average measurement outcome  $\langle O \rangle_{Q,\vec{j}}$  of the noisy and corrected

states  $\rho_{Q,j}$  approximates the noiseless measurement outcome.

To measure the average outcome to an additive error  $\varepsilon$  with failure probability  $\delta$ , we need  $T \propto C^2 \log(\delta^{-1})/\varepsilon^2$  samples according to the Hoeffding inequality. Since the number of samples needed given access to  $\rho_I(T)$  is  $T_0 \propto \log(\delta^{-1})/\varepsilon^2$ , the error mitigation scheme introduces a sampling overhead  $C^2$ , which can be regarded as a resource cost for the stochastic QEM scheme. The overhead scales as  $C^2(T) = \exp(\mathcal{O}(\lambda T))$  given noisy strength  $\lambda$  and evolution time  $T$ . Here we choose a normalisation  $\lambda$  so that the contribution from  $\mathcal{L}_{\text{exp}}$  is bounded by a constant. Therefore the condition that the scheme works efficiently with a constant resource cost is  $\lambda T = \mathcal{O}(1)$ . By regarding  $\lambda$  as the error rate, the condition can be intuitively interpreted as that the total noise rate is a constant, aligning with the result for conventional QEM. We will presently discuss the magnitude of the overhead with NISQ devices and refer to [37] for details.

*Stochastic QEM.*— In practice, it could be challenging to ‘continuously’ interchange the noisy evolution and the recovery operation within a sufficiently small time step  $\delta t$ . Since  $\mathcal{E}_I(t) \approx \mathcal{E}_N(t)$  and the recovery operation at each time is almost an identity operation

$$\mathcal{E}_Q = c \left( p_0 \mathcal{I} + \sum_{j \geq 1} \alpha_j \tilde{p}_j \delta t \mathcal{B}_j \right), \quad (7)$$

with  $\mathcal{B}_0$  being the identity channel  $\mathcal{I}$ ,  $p_0 = 1 - \mathcal{O}(\delta t)$ , and  $\tilde{p}_j = p_j/\delta t = \mathcal{O}(1)$ , we can further apply the Monte Carlo method to stochastically realise the continuous recovery operations as shown in Fig. 1(b). Specifically, we initialise  $\alpha = 1$  and randomly generate  $q \in [0, 1]$  at time  $t = 0$ . Then evolve the state according to the noisy evolution  $\mathcal{E}_N$  until time  $t_{\text{jp}}$  by solving  $p(t_{\text{jp}}) = q$  with  $p(t) = \exp(-\Gamma(t))$  and  $\Gamma(t) = t \sum_{j \geq 1} \tilde{p}_j$ . At time  $t_{\text{jp}}$ , we generate another uniformly distributed random number  $q' \in [0, 1]$ , apply the recovery operation  $\mathcal{B}_j$  if  $q' \in [s_{j-1}, s_j]$ , and update the coefficient as  $\alpha = \alpha_j \alpha$ . Here  $s_j(t) = (\sum_{i=1}^j \tilde{p}_i)/(\sum_{i=1}^{N_{\text{op}}} \tilde{p}_i)$ ,  $N_{\text{op}}$  is the number of basis operations, and the sum omits the identity channel. Then, we randomly initialise  $q$ , and repeat this procedure until time reaches  $T$ . On average, we prove that the *stochastic* QEM scheme is equivalent to the ‘continuous’ one [37]. While differently, the stochastic QEM does not assume time discretisation and it only requires to randomly apply a few recovery operations, scaling as  $\mathcal{O}(\lambda T)$  [37]. We can insert the recovery operations by ‘pausing’ the original noisy evolution. Alternatively, since we can determine the time  $t_{\text{jp}}$  and the recovery operations before the experiment, they can be pre-engineered into the original evolution. Therefore, we can effectively implement stochastic QEM via the noisy time evolution of Eq. (2) with an adjusted Hamiltonian. We summarise the scheme as follows.

---

**Algorithm 1** Stochastic error mitigation.

---

Input: initial state  $\rho(0)$ , number of samples  $N_s$ , noisy evolution  $\mathcal{E}_N$ , basis operations  $\mathcal{B}_j$ ; Output:  $\bar{O}$ .

---

```

1: Get  $C$ ,  $\{\alpha_j\}$ , and  $\{p_j\}$  of Eq. (29), set  $\left\{s_j = \frac{\sum_{i=1}^j \tilde{p}_i}{\sum_{i=1}^{N_{\text{op}}} \tilde{p}_i}\right\}$ .
2: for  $m = 1$  to  $N_s$  do
3:   Randomly generate  $q_0 \in [0, 1]$ , set  $t = 0$ ,  $n = 0$ ,  $\alpha = 1$ .
4:   while  $t \leq T$  do
5:     Get  $t_{\text{jp}}^n$  by solving  $\exp(-\Gamma(t_{\text{jp}}^n)) = q_n$ .
6:     Randomly generate  $q'_n \in [0, 1]$ .
7:     Set  $j_n = j$  if  $q'_n \in [s_{j-1}, s_j]$  and update  $\alpha = \alpha_{j_n} \cdot \alpha$ .
8:     Update  $t = t + t_{\text{jp}}^n$  and  $n = n + 1$ .
9:   end while
10:  Set  $\rho_Q = \rho(0)$  and  $\bar{O} = 0$ .
11:  for  $k = 0 : n - 1$  do
12:    Evolve  $\rho_Q$  under  $\mathcal{E}_N$  for time  $t_{\text{jp}}^k$  and apply  $\mathcal{B}_{j_k}$ .
13:  end for
14:  Evolve  $\rho_Q$  under  $\mathcal{E}_N$  for time  $T - \sum_{k=0}^{n-1} t_{\text{jp}}^k$ .
15:  Measure  $O$  of  $\rho_Q$  to get  $O_m$ .
16:  Update  $\bar{O} = \bar{O} + C \alpha O_m / N_s$ 
17: end for

```

---

*Reduction of model estimation error.*— While the above QEM schemes assume a prior knowledge of the noise model, the realistic noise  $\mathcal{L}_{\text{exp}}$  and the estimated noise  $\mathcal{L}_{\text{est}}$  may differ due to imprecise estimation of the noise model. Here we combine the extrapolation QEM method [3, 4] to further mitigate such model estimation errors. The effective evolution after applying the error mitigation method with  $\mathcal{L}_{\text{est}}$  is

$$\frac{d}{dt} \rho_{\lambda}^{(Q)}(t) = -i[H(t), \rho_{\lambda}^{(Q)}(t)] + \lambda \Delta \mathcal{L}[\rho_{\lambda}^{(Q)}(t)], \quad (8)$$

where  $\rho_{\lambda}^{(Q)}(t)$  is the effective density matrix and  $\Delta \mathcal{L} = \mathcal{L}_{\text{exp}} - \mathcal{L}_{\text{est}}$ . By re-scaling  $H(t) \rightarrow \frac{1}{r} H(\frac{t}{r})$ , the evolution for rescaled time  $rt$  is

$$\frac{d}{dt} \rho_{r\lambda}^{(Q)}(t) = -i[H(t), \rho_{r\lambda}^{(Q)}(t)] + r\lambda \Delta \mathcal{L}[\rho_{r\lambda}^{(Q)}(t)], \quad (9)$$

which can be implemented by re-running the error-mitigated experiment with re-scaled Hamiltonian and time. As the value of  $r \geq 1$  can be tuned, we choose several different values of  $r$  and suppress the model estimation error via Richardson extrapolation. Specifically, with more than two values of  $r$  denoted as  $\{r_j\}$  and constants  $\beta_j = \prod_{l \neq j} r_l (r_l - r_j)^{-1}$ , we have

$$\langle O \rangle_I = \sum_{j=0}^n \beta_j \langle O \rangle_{r_j \lambda} + \mathcal{O} \left( \frac{\gamma_n (r_{\text{max}} \lambda T \|\Delta \mathcal{L}\|_1)^{n+1}}{(n+1)!} \right). \quad (10)$$

with  $\rho_{r\lambda}^{(Q)}$  as  $\langle O \rangle_{r\lambda}$  being the error mitigated measurement outcome,  $\gamma_n = \sum_j |\beta_j|$ ,  $r_{\text{max}} = \max_j r_j$ , and  $\|\Delta \mathcal{L}\|_1 = \max_{\rho} \text{Tr}|\mathcal{L}(\rho)|$ . Therefore, in addition to  $\lambda T = \mathcal{O}(1)$ , the scheme is efficient provided  $r_{\text{max}} \|\Delta \mathcal{L}\|_1 = \mathcal{O}(1)$ . Note that, since imperfections of the basis operations  $\mathcal{B}_i$  also lead to deviation of  $\mathcal{L}_{\text{est}}$ , they can be

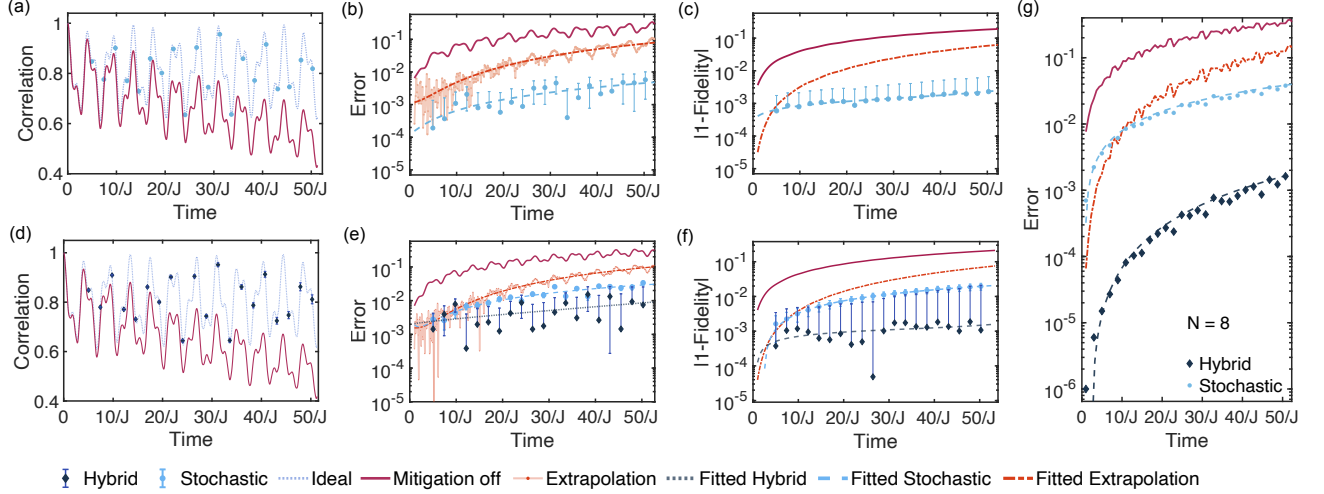


FIG. 2. Numerical test of the QEM schemes without ((a)(b)(c)) and with 10% model estimation error  $\lambda_{\text{exp}} = 1.1\lambda_{\text{est}}$  ((d)(e)(f)(g)). We consider the dynamics of 2D anisotropic Heisenberg Hamiltonian with energy relaxation and dephasing noise. (a)–(f) consider a four-qubit Hamiltonian with finite ( $10^6$ ) number of samples. (a) and (d) compares the time evolved nearest-neighbour correlation function  $\sum_{\langle ij \rangle} \sigma_x^{(i)} \sigma_x^{(j)} / 4$ . (b) and (e) shows the error between the exact value and the error-mitigated value. (c) and (f) shows the fidelity of the effective density matrix  $\rho_{\text{eff}}^\alpha$  and the ideal one  $\rho_I$  under different error mitigation scheme  $\alpha$ . (g) consider an eight-qubit Hamiltonian with infinite number of samples. The hybrid error mitigation scheme suppresses the error up to about four orders of magnitude even with 10% model estimation error.

corrected via the extrapolation procedure. We refer to [37] for detailed analyses.

*Numerical simulation.*— Now, we test our QEM schemes for analog quantum simulators and gate-based digital quantum circuits. We first consider a 2D anisotropic Heisenberg model  $H = J \sum_{\langle ij \rangle} [(1 + \gamma) \sigma_x^{(i)} \sigma_x^{(j)} + (1 - \gamma) \sigma_y^{(i)} \sigma_y^{(j)} + \sigma_z^{(i)} \sigma_z^{(j)}] - \gamma \hbar \sum_{i=1}^4 \sigma_y^{(i)}$  on a  $2 \times 2$  square lattice, where  $\langle ij \rangle$  represents nearest neighbour pairs. This model has been extensively used to investigate the quantum magnetism and criticality [76–80]. We consider analog simulation via a noisy superconducting quantum simulator with energy relaxation  $\mathcal{L}_1$  and dephasing  $\mathcal{L}_2$  noise [47, 81–83]. Here  $\mathcal{L}_\beta[\rho] = \sum_j \lambda_\beta (L_\beta^{(j)} \rho L_\beta^{(j)\dagger} - \frac{1}{2} \{L_\beta^{(j)\dagger} L_\beta^{(j)}, \rho\})$  for  $\beta = 1, 2$ ,  $L_1^{(j)} = \sigma_-^{(j)} = |0\rangle\langle 1|$ , and  $L_2^{(j)} = \sigma_z^{(j)}$ . Such a noise model is also relevant for other quantum simulators such as trapped ions [41, 50, 57, 74], NMR [45, 46, 49], ultracold atoms [52, 56], optical lattices apparatus [54], etc. The noise can be characterised by measuring energy relaxation time  $T_1$  and dephasing time  $T_2$  without full process tomography [61, 82–84] and more generally via local measurements [85, 86]. We also consider physical errors for the single-qubit recovery operations as single-qubit inhomogeneous Pauli error,  $\mathcal{E}_{\text{inh}} = (1 - p_x - p_y - p_z) \mathcal{I} + p_x \mathcal{X} + p_y \mathcal{Y} + p_z \mathcal{Z}$  with  $\mathcal{I}, \mathcal{X}, \mathcal{Y}, \mathcal{Z}$  being the Pauli channel and  $p_\alpha$  being the error probability. In our simulation, we set  $J = \hbar = 2\pi \times 4$  MHz,  $\gamma = 0.25$ , and the noise strength  $\lambda_1 = \lambda_2 = 0.04$  MHz [30, 61, 83].

For model estimation error, we set  $p_x = p_y = 0.25\%$  and  $p_z = 0.5\%$ , which can be achieved with current superconducting simulators [29, 87], and consider the real noise strength to be 10% greater than the estimated one, i.e.,  $\lambda_{\text{exp}} = 1.1\lambda_{\text{est}}$ . We set the initial state to  $(|+\rangle)^{\otimes 4}$  with  $|+\rangle = (|0\rangle + |1\rangle)/\sqrt{2}$ , evolve it to time  $T = 16\pi/J$ , and measure the expectation value of the normalised nearest-neighbour correlation function  $\sum_{\langle ij \rangle} \sigma_x^{(i)} \sigma_x^{(j)} / 4$  with  $10^6$  samples.

The numerical result without model estimation error is shown in Fig. 2 (a)(b)(c). Specifically, we compare the time evolution of the expectation value of the correlation operator in Fig. 2 (a)(b) and the fidelity  $F(\rho_I, \rho_{\text{eff}}) = \text{Tr} \sqrt{\rho_{\text{eff}}^{1/2} \rho_I \rho_{\text{eff}}^{1/2}}$  of the effective density matrix  $\rho_{\text{eff}}$  and the ideal one  $\rho_I$  in Fig. 2 (c). We can see that Richardson extrapolation and stochastic QEM improve the accuracy by one and two orders, respectively. The result with model estimation error is shown in Fig. 2 (d)(e)(f). Here, we also consider the hybrid method with both stochastic QEM and linear extrapolation, with optimised  $r_0 = 1$  and  $r_1 = 1.8$ . We can see that stochastic QEM still outperforms Richardson extrapolation with large evolution time and the hybrid method can be further used to improve the simulation accuracy. The simulation result thus indicates that the hybrid QEM scheme can be robust to the drift of noise [88–90]. The performance of the QEM schemes can be made clearer without considering sampling errors. As shown in Fig. 2(g), we consider simulations of the eight-qubit anisotropic Heisenberg model

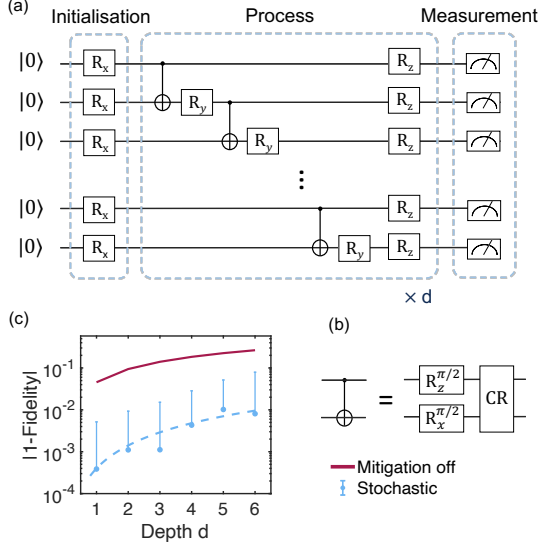


FIG. 3. Stochastic QEM for eight-qubit superconducting quantum circuits with environmental and crosstalk noise. (a) considers a  $d$ -depth parameterised quantum circuits with single-qubit rotations  $R_\alpha$  ( $\alpha \in \{X, Y, Z\}$ ) and CNOT gates. The rotation angles are randomly generated from  $[0, 2\pi]$ . (b) shows the realisation of the CNOT gate via the CR gate  $U_{CR} = \exp(i\pi\sigma_z^{(c)}\sigma_x^{(t)}/4)$  and single-qubit gates  $R_z^{\pi/2}$  and  $R_x^{\pi/2}$  up to a global phase  $e^{i\pi/4}$ . (c) shows the fidelity dependence of circuit depth  $d$  with/without QEM.

on  $2 \times 4$  lattice under different QEM schemes with infinite samples. The result indicates that both stochastic and hybrid QEM can effectively eliminate the accumulation of errors during the evolution.

Next, we consider a eight-qubit,  $d$ -depth parameterised quantum circuit (Fig. 3(c)) and show how stochastic QEM can suppress coherent errors in multi-qubit operations. Here, the controlled-NOT (CNOT) gate in the quantum circuits is generated by cross-resonance (CR) gates, which are experimentally realised by using microwaves to drive the control qubit ( $c$ ) at the frequency of the target qubit ( $t$ ), resulting in a driving Hamiltonian  $H \approx \Omega(-\sigma_z^{(c)}\sigma_x^{(t)} + \gamma\mathbb{I}^{(c)}\sigma_x^{(t)})$  [28, 30, 34–36]. Here,  $\Omega$  is the effective qubit-qubit coupling and  $\gamma$  represents the effect of crosstalk between qubits [34]. We consider inherent environmental noise and recovery operation error as in the above analog simulator, and additional coherent crosstalk errors  $\gamma = 1\%$ . We set  $\Omega = 2\pi$  MHz, the evolution time  $T = \pi/4\Omega$ , and run  $10^5$  samples. We mitigate the noisy two-qubit pulse sequence by inserting basis operations, and shows the fidelity dependence of circuit depth  $d$  with/without QEM in Fig. 3(c). The result clearly shows that stochastic QEM improves the computing accuracy by two orders.

In [37], we show numerical simulations for both Ising and frustrated quantum spin Hamiltonian and demonstrate how the QEM methods can be applied to tempo-

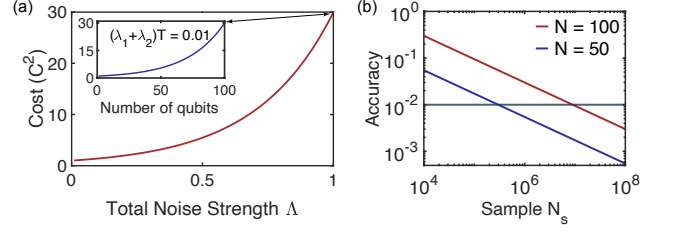


FIG. 4. (a) Cost versus total noise strength  $\Lambda = NT(\lambda_1 + \lambda_2)$ . We consider a general  $N$ -qubit Hamiltonian  $H_{\text{sim}}$  with single-qubit energy relaxation ( $\lambda_1$ ) and dephasing noise ( $\lambda_2 = \lambda_1$ ), and evolution time  $T$ . The inset shows the cost versus different number of qubits with  $(\lambda_1 + \lambda_2)T = 0.01$ . (b) Simulation accuracy  $\varepsilon \propto C/\sqrt{N_s}$  with different number of samples  $N_s$  with  $T = 1 \mu\text{s}$ ,  $\lambda_1 + \lambda_2 = 0.01$  MHz,  $N = 100$  (red) and  $N = 50$  (blue). We only consider pessimistic estimation  $C/\sqrt{N_s}$  and the error  $\varepsilon$  can be much smaller in practice.

rally correlated noise.

*Resource cost for NISQ devices.*— We estimate the resource cost for stochastic error mitigation with NISQ devices. Given precise noise model, the stochastic error mitigation method in principle enables exact recovery of the ideal evolution. However, to achieve the same accuracy of the measurement on the ideal evolution, we need  $C^2$  times more samples or experiment runs with the error-mitigated noisy evolution. The overhead  $C^2$  is likely to be prohibitively large with a significant amount of noise on a NISQ device. Nevertheless, we show that the overhead can be reasonably small (less than 100) when the total error (defined below) is less than 1. In particular, we consider a noisy superconducting simulator with up to  $N = 100$  qubits, which suffers from single-qubit relaxation and dephasing noise with equal noise strength  $\lambda_1 = \lambda_2$ . While the noise strength is defined as the noise rate at instant time, we define the total noise strength  $\Lambda = NT(\lambda_1 + \lambda_2)$  as the noise strength of the whole  $N$ -qubit system within time  $T$ . The dependence of the overhead  $C^2$  on the total noise strength  $\Lambda$  and number of qubits is shown in Fig. 4(a). For a practical case with  $T = 1 \mu\text{s}$ ,  $\lambda_1 + \lambda_2 = 0.01$  MHz,  $N = 100$ , the cost  $C^2(\Lambda = 1) = 30$  and we further show the number of measurements needed to achieve a given simulation accuracy in Fig. 4(b). Note that the overhead  $C^2$  is independent of the Hamiltonian  $H_{\text{sim}}$ , so the results apply for general NISQ devices [37].

*Discussion.*— To summarise, we propose quantum error mitigation schemes for a continuous process. We numerically test it with several analog simulators under energy relaxing and dephasing noise and a quantum circuit under additional crosstalk noise. We show its feasibility with general NISQ devices with up to 100 qubits. The proposed QEM schemes work for all digital and many analog quantum simulators with accurate

single-qubit controls. Since dominant noise in NISQ devices is from implementing multi-qubit operations or inherent noise with finite coherence time, our scheme can effectively suppress them and thus extend the computation capability of NISQ devices in solving practical problems [29]. Furthermore, resolving the drift of noise is challenging for conventional QEM methods. Our hybrid scheme can mitigate model estimation error and is tested to be robust to the drift of noise.

*Acknowledgements.* — SE and JS acknowledge Yuichiro Matsuzaki, Hideaki Hakoshima, Tianhan Liu and Shuxiang Cao for useful discussions. SE acknowledges financial support from the Japan Student Services Organization (JASSO) Student Exchange Support Program (Graduate Scholarship for Degree Seeking Students). TT acknowledges financial support from the Masason Foundation. XY and SCB acknowledges EPSRC projects EP/M013243/1 and the European Quantum Technology Flagship project AQTION. VV thanks the National Research Foundation, Prime Ministers Office, Singapore, under its Competitive Research Programme (CRP Award No. NRF- CRP14-2014-02) and administered by Centre for Quantum Technologies, National University of Singapore.

---

\* jinzhaosun@physics.ox.ac.uk

† xiao.yuan.ph@gmail.com

‡ suguru.endou.uc@hco.ntt.co.jp

- [1] F. Arute, K. Arya, R. Babbush, D. Bacon, J. C. Bardin, R. Barends, R. Biswas, S. Boixo, F. G. Brandao, D. A. Buell, *et al.*, *Nature* **574**, 505 (2019).
- [2] J. Preskill, *Quantum* **2**, 79 (2018).
- [3] Y. Li and S. C. Benjamin, *Physical Review X* **7**, 021050 (2017).
- [4] K. Temme, S. Bravyi, and J. M. Gambetta, *Physical review letters* **119**, 180509 (2017).
- [5] S. Endo, S. C. Benjamin, and Y. Li, *Physical Review X* **8**, 031027 (2018).
- [6] J. R. McClean, M. E. Kimchi-Schwartz, J. Carter, and W. A. de Jong, *Phys. Rev. A* **95**, 042308 (2017).
- [7] M. Huo and Y. Li, *arXiv preprint arXiv:1811.02734* (2018).
- [8] X. Bonet-Monroig, R. Sagastizabal, M. Singh, and T. O'Brien, *Physical Review A* **98**, 062339 (2018).
- [9] E. F. Dumitrescu, A. J. McCaskey, G. Hagen, G. R. Jansen, T. D. Morris, T. Papenbrock, R. C. Pooser, D. J. Dean, and P. Lougovski, *Physical review letters* **120**, 210501 (2018).
- [10] M. Otten and S. K. Gray, *Physical Review A* **99**, 012338 (2019).
- [11] S. McArdle, X. Yuan, and S. Benjamin, *Physical review letters* **122**, 180501 (2019).
- [12] R. Sagastizabal, X. Bonet-Monroig, M. Singh, M. A. Rol, C. Bultink, X. Fu, C. Price, V. Ostroukh, N. Muthusubramanian, A. Bruno, *et al.*, *Physical Review A* **100**, 010302 (2019).
- [13] W. J. Huggins, J. McClean, N. Rubin, Z. Jiang, N. Wiebe, K. B. Whaley, and R. Babbush, *arXiv preprint arXiv:1907.13117* (2019).
- [14] J. I. Colless, V. V. Ramasesh, D. Dahlen, M. S. Blok, M. E. Kimchi-Schwartz, J. R. McClean, J. Carter, W. A. de Jong, and I. Siddiqi, *Phys. Rev. X* **8**, 011021 (2018).
- [15] M. Otten and S. K. Gray, *Npj Quantum Inf.* **5**, 11 (2019).
- [16] J. R. McClean, Z. Jiang, N. C. Rubin, R. Babbush, and H. Neven, *Nature Communications* **11**, 1 (2020).
- [17] T. Giurgica-Tiron, Y. Hindy, R. LaRose, A. Mari, and W. J. Zeng, *arXiv preprint arXiv:2005.10921* (2020).
- [18] T. Keen, T. Maier, S. Johnston, and P. Lougovski, *Quantum Science and Technology* **5**, 035001 (2020).
- [19] Z. Cai, *arXiv preprint arXiv:2007.01265* (2020).
- [20] A. He, B. Nachman, W. A. de Jong, and C. W. Bauer, *arXiv preprint arXiv:2003.04941* (2020).
- [21] F. B. Maciejewski, Z. Zimborás, and M. Oszmaniec, *Quantum* **4**, 257 (2020).
- [22] Y. Chen, M. Farahzad, S. Yoo, and T.-C. Wei, *Physical Review A* **100**, 052315 (2019).
- [23] H. Kwon and J. Bae, *arXiv preprint arXiv:2003.12314* (2020).
- [24] A. Strikis, D. Qin, Y. Chen, S. C. Benjamin, and Y. Li, *arXiv preprint arXiv:2005.07601* (2020).
- [25] S. Bravyi, S. Sheldon, A. Kandala, D. C. McKay, and J. M. Gambetta, *arXiv preprint arXiv:2006.14044* (2020).
- [26] P. Czarnik, A. Arrasmith, P. J. Coles, and L. Cincio, *arXiv preprint arXiv:2005.10189* (2020).
- [27] A. Zlokapa and A. Gheorghiu, *arXiv preprint arXiv:2005.10811* (2020).
- [28] A. Kandala, K. Temme, A. D. Córcoles, A. Mezzacapo, J. M. Chow, and J. M. Gambetta, *Nature* **567**, 491 (2019).
- [29] M. Kjaergaard, M. E. Schwartz, J. Braumüller, P. Krantz, J. I.-J. Wang, S. Gustavsson, and W. D. Oliver, *arXiv preprint arXiv:1905.13641* (2019).
- [30] P. Krantz, M. Kjaergaard, F. Yan, T. P. Orlando, S. Gustavsson, and W. D. Oliver, *Applied Physics Reviews* **6**, 021318 (2019).
- [31] S. Sheldon, E. Magesan, J. M. Chow, and J. M. Gambetta, *Physical Review A* **93**, 060302 (2016).
- [32] J. Plantenberg, P. De Groot, C. Harmans, and J. Mooij, *Nature* **447**, 836 (2007).
- [33] C. Neill, P. Roushan, K. Kechedzhi, S. Boixo, S. V. Isakov, V. Smelyanskiy, A. Megrant, B. Chiaro, A. Dunsworth, K. Arya, *et al.*, *Science* **360**, 195 (2018).
- [34] A. D. Córcoles, J. M. Gambetta, J. M. Chow, J. A. Smolin, M. Ware, J. Strand, B. L. Plourde, and M. Steffen, *Physical Review A* **87**, 030301 (2013).
- [35] J. M. Chow, J. M. Gambetta, A. D. Córcoles, S. T. Merkel, J. A. Smolin, C. Rigetti, S. Poletto, G. A. Keefe, M. B. Rothwell, J. R. Rozen, *et al.*, *Physical review letters* **109**, 060501 (2012).
- [36] C. Rigetti and M. Devoret, *Physical Review B* **81**, 134507 (2010).
- [37] See Supplemental Materials for analytical results and implementation details.
- [38] M. Takita, A. W. Cross, A. Córcoles, J. M. Chow, and J. M. Gambetta, *Physical review letters* **119**, 180501 (2017).
- [39] M. Reagor, C. B. Osborn, N. Tezak, A. Staley, G. Prawiroatmodjo, M. Scheer, N. Alidoust, E. A. Sete, N. Didier, M. P. da Silva, *et al.*, *Science advances* **4**, eaao3603 (2018).



- [40] J. Eisert, M. Friesdorf, and C. Gogolin, *Nature Physics* **11**, 124 (2015).
- [41] J. G. Bohnet, B. C. Sawyer, J. W. Britton, M. L. Wall, A. M. Rey, M. Foss-Feig, and J. J. Bollinger, *Science* **352**, 1297 (2016).
- [42] S. An, J.-N. Zhang, M. Um, D. Lv, Y. Lu, J. Zhang, Z.-Q. Yin, H. Quan, and K. Kim, *Nature Physics* **11**, 193 (2015).
- [43] P. Schindler, M. Müller, D. Nigg, J. T. Barreiro, E. A. Martinez, M. Hennrich, T. Monz, S. Diehl, P. Zoller, and R. Blatt, *Nature Physics* **9**, 361 (2013).
- [44] K. A. Landsman, C. Figgatt, T. Schuster, N. M. Linke, B. Yoshida, N. Y. Yao, and C. Monroe, *Nature* **567**, 61 (2019).
- [45] J. Li, R. Fan, H. Wang, B. Ye, B. Zeng, H. Zhai, X. Peng, and J. Du, *Physical Review X* **7**, 031011 (2017).
- [46] M. Gärttner, J. G. Bohnet, A. Safavi-Naini, M. L. Wall, J. J. Bollinger, and A. M. Rey, *Nature Physics* **13**, 781 (2017).
- [47] A. A. Houck, H. E. Türeci, and J. Koch, *Nature Physics* **8**, 292 (2012).
- [48] R. Harris, Y. Sato, A. Berkley, M. Reis, F. Altomare, M. Amin, K. Boothby, P. Bunyk, C. Deng, C. Enderud, *et al.*, *Science* **361**, 162 (2018).
- [49] Z. Li, H. Zhou, C. Ju, H. Chen, W. Zheng, D. Lu, X. Rong, C. Duan, X. Peng, and J. Du, *Physical review letters* **112**, 220501 (2014).
- [50] A. Friedenauer, H. Schmitz, J. T. Glueckert, D. Porras, and T. Schätz, *Nature Physics* **4**, 757 (2008).
- [51] J. Zhang, G. Pagano, P. W. Hess, A. Kyprianidis, P. Becker, H. Kaplan, A. V. Gorshkov, Z.-X. Gong, and C. Monroe, *Nature* **551**, 601 (2017).
- [52] R. A. Hart, P. M. Duarte, T.-L. Yang, X. Liu, T. Paiva, E. Khatami, R. T. Scalettar, N. Trivedi, D. A. Huse, and R. G. Hulet, *Nature* **519**, 211 (2015).
- [53] Z.-X. Gong and L.-M. Duan, *New Journal of Physics* **15**, 113051 (2013).
- [54] J. Struck, C. Ölschläger, R. Le Targat, P. Soltan-Panahi, A. Eckardt, M. Lewenstein, P. Windpassinger, and K. Sengstock, *Science* **333**, 996 (2011).
- [55] Y.-L. Wu and S. D. Sarma, *Physical Review A* **93**, 022332 (2016).
- [56] H. Bernien, S. Schwartz, A. Keesling, H. Levine, A. Omran, H. Pichler, S. Choi, A. S. Zibrov, M. Endres, M. Greiner, *et al.*, *Nature* **551**, 579 (2017).
- [57] P. Jurcevic, H. Shen, P. Hauke, C. Maier, T. Brydges, C. Hempel, B. Lanyon, M. Heyl, R. Blatt, and C. Roos, *Physical review letters* **119**, 080501 (2017).
- [58] E. Altman, K. R. Brown, G. Carleo, L. D. Carr, E. Demler, C. Chin, B. DeMarco, S. E. Economou, M. Eriksson, K.-M. C. Fu, *et al.*, *arXiv preprint arXiv:1912.06938* (2019).
- [59] I. M. Georgescu, S. Ashhab, and F. Nori, *Reviews of Modern Physics* **86**, 153 (2014).
- [60] P. Hauke, F. M. Cucchietti, L. Tagliacozzo, I. Deutsch, and M. Lewenstein, *Reports on Progress in Physics* **75**, 082401 (2012).
- [61] J. Bylander, S. Gustavsson, F. Yan, F. Yoshihara, K. Harrabi, G. Fitch, D. G. Cory, Y. Nakamura, J.-S. Tsai, and W. D. Oliver, *Nature Physics* **7**, 565 (2011).
- [62] P. Bertet, I. Chiorescu, G. Burkard, K. Semba, C. Harman, D. P. DiVincenzo, and J. Mooij, *Physical review letters* **95**, 257002 (2005).
- [63] J. M. Martinis, S. Nam, J. Aumentado, K. Lang, and C. Urbina, *Physical Review B* **67**, 094510 (2003).
- [64] A. Walther, F. Ziesel, T. Ruster, S. T. Dawkins, K. Ott, M. Hettrich, K. Singer, F. Schmidt-Kaler, and U. Poschinger, *Physical review letters* **109**, 080501 (2012).
- [65] B. Pokharel, N. Anand, B. Fortman, and D. A. Lidar, *Physical review letters* **121**, 220502 (2018).
- [66] T. P. Harty, D. T. C. Allcock, C. J. Ballance, L. Guidoni, H. A. Janacek, N. M. Linke, D. N. Stacey, and D. M. Lucas, *Phys. Rev. Lett.* **113**, 220501 (2014).
- [67] C. J. Ballance, T. P. Harty, N. M. Linke, M. A. Sepiol, and D. M. Lucas, *Phys. Rev. Lett.* **117**, 060504 (2016).
- [68] J. P. Gaebler, T. R. Tan, Y. Lin, Y. Wan, R. Bowler, A. C. Keith, S. Glancy, K. Coakley, E. Knill, D. Leibfried, and D. J. Wineland, *Phys. Rev. Lett.* **117**, 060505 (2016).
- [69] A. Mezzacapo, U. Las Heras, J. Pedernales, L. DiCarlo, E. Solano, and L. Lamata, *Scientific reports* **4**, 1 (2014).
- [70] L. García-Álvarez, J. Casanova, A. Mezzacapo, I. Egusquiza, L. Lamata, G. Romero, and E. Solano, *Physical review letters* **114**, 070502 (2015).
- [71] S. Asaad, C. Dickel, N. K. Langford, S. Poletto, A. Bruno, M. A. Rol, D. Deurloo, and L. DiCarlo, *npj Quantum Information* **2**, 1 (2016).
- [72] S. J. Weber, G. O. Samach, D. Hover, S. Gustavsson, D. K. Kim, A. Melville, D. Rosenberg, A. P. Sears, F. Yan, J. L. Yoder, *et al.*, *Physical Review Applied* **8**, 014004 (2017).
- [73] H. Häffner, W. Hänsel, C. Roos, J. Benhelm, M. Chwalla, T. Körber, U. Rapol, M. Riebe, P. Schmidt, C. Becher, *et al.*, *Nature* **438**, 643 (2005).
- [74] R. Blatt and C. F. Roos, *Nature Physics* **8**, 277 (2012).
- [75] M. Saffman, *Journal of Physics B: Atomic, Molecular and Optical Physics* **49**, 202001 (2016).
- [76] M. H. Lee, I. Kim, and R. Dekeyser, *Physical review letters* **52**, 1579 (1984).
- [77] L. Siurakshina, D. Ihle, and R. Hayn, *Physical Review B* **61**, 14601 (2000).
- [78] A. Hucht, A. Moschel, and K. Usadel, *Journal of magnetism and magnetic materials* **148**, 32 (1995).
- [79] D. Torelli and T. Olsen, *2D Materials* **6**, 015028 (2018).
- [80] C. Soukoulis, S. Datta, and Y. H. Lee, *Physical Review B* **44**, 446 (1991).
- [81] L. Lamata, A. Parra-Rodriguez, M. Sanz, and E. Solano, *Advances in Physics: X* **3**, 1457981 (2018).
- [82] W. D. Oliver and P. B. Welander, *MRS bulletin* **38**, 816 (2013).
- [83] X. Gu, A. F. Kockum, A. Miranowicz, Y.-x. Liu, and F. Nori, *Physics Reports* **718**, 1 (2017).
- [84] Z. Zhou, S.-I. Chu, and S. Han, *Journal of Physics B: Atomic, Molecular and Optical Physics* **41**, 045506 (2008).
- [85] E. Bairey, C. Guo, D. Poletti, N. H. Lindner, and I. Arad, *New Journal of Physics* **22**, 032001 (2020).
- [86] M. P. da Silva, O. Landon-Cardinal, and D. Poulin, *Natural Review Letters* **107**, 210404 (2011).
- [87] N. M. Linke, D. Maslov, M. Roetteler, S. Debnath, C. Figgatt, K. A. Landsman, K. Wright, and C. Monroe, *Proceedings of the National Academy of Sciences* **114**, 3305 (2017).
- [88] C. Müller, J. Lisenfeld, A. Shnirman, and S. Poletto, *Physical Review B* **92**, 035442 (2015).
- [89] S. M. Meißner, A. Seiler, J. Lisenfeld, A. V. Ustinov, and

- G. Weiss, Physical Review B **97**, 180505 (2018).
- [90] C. Neill, A. Megrant, R. Barends, Y. Chen, B. Chiaro, J. Kelly, J. Mutus, P. O'Malley, D. Sank, J. Wenner, *et al.*, Applied Physics Letters **103**, 072601 (2013).
- [91] D. Greenbaum, arXiv preprint arXiv:1509.02921 (2015).
- [92] J. T. Barreiro, M. Müller, P. Schindler, D. Nigg, T. Monz, M. Chwalla, M. Hennrich, C. F. Roos, P. Zoller, and R. Blatt, Nature **470**, 486 (2011).
- [93] R. F. Bishop, D. J. Farnell, and J. B. Parkinson, Physical Review B **58**, 6394 (1998).
- [94] Y. Matsuzaki, S. C. Benjamin, and J. Fitzsimons, Physical Review A **84**, 012103 (2011).
- [95] Y. Matsuzaki, S. Saito, K. Kakuyanagi, and K. Semba, Physical Review B **82**, 180518 (2010).
- [96] K. Kakuyanagi, T. Meno, S. Saito, H. Nakano, K. Semba, H. Takayanagi, F. Deppe, and A. Shnirman, Physical review letters **98**, 047004 (2007).
- [97] F. Yoshihara, K. Harrabi, A. Niskanen, Y. Nakamura, and J. S. Tsai, Physical review letters **97**, 167001 (2006).

## SUPPLEMENTAL MATERIALS: MITIGATING REALISTIC NOISE IN PRACTICAL NOISY INTERMEDIATE-SCALE QUANTUM DEVICES

### QUANTUM ERROR MITIGATION FOR GATED-BASED QUANTUM COMPUTING

#### Error Model

Here we review the concept of quantum error mitigation (QEM) for digital quantum computing. In a digital gate-based quantum computer, the effect of noise is simplified as a quantum channel appearing either before or after each gate. The output state is different from the ideal output, which can be described as

$$\begin{aligned}\rho_{\text{out}}^{\text{noisy}} &= \mathcal{N}_{N_g} \circ \mathcal{U}_{N_g} \circ \dots \mathcal{N}_1 \circ \mathcal{U}_1(\rho_{\text{in}}) \\ \rho_{\text{out}}^{\text{ideal}} &= \mathcal{U}_{N_g} \circ \dots \circ \mathcal{U}_1(\rho_{\text{in}}),\end{aligned}\tag{11}$$

where  $\rho_{\text{out}}^{\text{noisy}}$  is a noisy output and  $\rho_{\text{out}}^{\text{ideal}}$  is a noise-free output from the quantum circuit,  $\mathcal{U}_k$  and  $\mathcal{N}_k$  are  $k^{\text{th}}$  quantum operation and accompanying noise to it, and  $N_g$  is the number of gates. Here, we assume the noise processes are Markovian for simplicity. Fault-tolerant error correction based on encoding of qubits can be used to compensate for the effect of noise and obtain correct computation results in principle. However, in near-term quantum computing, the number of qubits and gate operations are restricted due to imperfections of quantum devices including physical noise and limited interactions among qubits. Therefore, fault-tolerant error correction necessitating encoding of qubits is not ideal for near-term quantum computing. Instead, QEM was introduced for mitigating errors in quantum circuits without using additional qubits. By using QEM, one cannot restore the quantum state itself, but can instead obtain an approximation of expected values of observables corresponding to the ideal density matrix, i.e.,

$$\text{Tr} \left[ \text{QEM} \left( \rho_{\text{out}}^{\text{noisy}} \right) O \right] \approx \text{Tr} \left[ \rho_{\text{out}}^{\text{ideal}} O \right],\tag{12}$$

for any observable  $O$ . Here we use  $\text{QEM}(\rho)$  to denote the process of error mitigation, which may not satisfy the requirements of a quantum channel. Therefore, we generally need a classical post-processing to realise  $\text{QEM}(\rho)$ , which may introduce a sampling overhead (cost) when measuring observables. The cost in general increases exponentially with respect to the error strength as we shortly see below. Therefore, a constant error strength is generally required in order to make QEM to work.

#### Quasi-probability method

Among different QEM schemes via different post-processing mechanisms, the quasi-probability error mitigation method is one of the most effective techniques. It recovers the ideal unitary processes by randomly generating noisy operations, with post processing of measurement results. Suppose the ideal quantum operation is denoted as  $\mathcal{U}$ , then the key idea of the quasi-probability method is to express the ideal evolution  $\mathcal{U}$  as a linear combination of noisy operations  $\mathcal{K}_i$  as

$$\mathcal{U} \approx \sum_i q_i \mathcal{K}_i = C \sum_i p_i \text{sgn}(q_i) \mathcal{K}_i,\tag{13}$$



where  $\mathcal{U}$  and  $\mathcal{K}_i$  are superoperators, and  $\sum_i q_i = 1$ ,  $C = \sum_i |q_i|$ ,  $p_i = |q_i|/C$ . As  $q_i$  can be negative, we refer to  $q_i$  as the quasi-probability, and therefore the overhead coefficient  $C \geq 1$  in general. To obtain the error free expectation value of an observable  $O$ , we randomly generate noisy operation  $\mathcal{K}_i$  with probability  $p_i$ , multiply the measured result by the parity factor  $\text{sgn}(q_i)$ , and obtain the expectation value  $\langle O \rangle_{\text{eff}}$  as follows,

$$\langle O \rangle_{\text{eff}} = \sum_i p_i \text{sgn}(q_i) \text{Tr}[O \mathcal{K}_i(\rho_{\text{in}})], \quad (14)$$

Finally, the error free expectation value of  $\langle O \rangle$  is approximated by  $C \langle O \rangle_{\text{eff}}$ . Note that the variance is amplified  $C^2$  times greater, and thus  $C^2$  can be interpreted as a resource cost to achieve the same accuracy as that without QEM.

As an example, we illustrate the case that the single qubit operation is affected by depolarising errors as  $\mathcal{DU}$ . The removal of the error  $\mathcal{D}$  can be formally done by applying its inverse channel  $\mathcal{D}^{-1}$ . Now, the depolarising channel can be expressed as

$$\mathcal{D}(\rho) = \left(1 - \frac{3}{4}p\right) \rho + \frac{p}{4}(X\rho X + Y\rho Y + Z\rho Z), \quad (15)$$

with the inverse channel derived as

$$\mathcal{D}^{-1}(\rho) = C_{\mathcal{D}^{-1}}[p_1\rho - p_2(X\rho X + Y\rho Y + Z\rho Z)], \quad (16)$$

where  $C_{\mathcal{D}^{-1}} = (p+2)/(2-2p) > 1$ ,  $p_1 = (4-p)/(2p+4)$ , and  $p_2 = p/(2p+4)$ .

Consequently, the ideal channel  $\mathcal{U}$  can be expressed as

$$\begin{aligned} \mathcal{U} &= \mathcal{D}^{-1}\mathcal{DU} \\ &= C_{\mathcal{D}^{-1}}[p\mathcal{I}\mathcal{DU} - p_2(\mathcal{X}\mathcal{DU} + \mathcal{Y}\mathcal{DU} + \mathcal{Z}\mathcal{DU})], \end{aligned} \quad (17)$$

where  $\mathcal{I}$ ,  $\mathcal{X}$ ,  $\mathcal{Y}$  and  $\mathcal{Z}$  correspond to an identity operation, and superoperators for Pauli operators. Note that Eq. (17) is written in the same form as Eq. (13), and we can hence perform the quasi-probability method accordingly.

For the error mitigation method to be useful in digital quantum computing, this quasi-probability operation is applied after each noisy gate. The parity is updated depending on the generated operations, and the final outcome of the parity is applied to measurement results in the same way as a single quantum operation shown in Eq. (13). Suppose there are  $N$  gates, the total overhead  $C_N$  can be expressed as

$$C_N = \prod_{i=1}^N C_i, \quad (18)$$

where  $C_i$  is the overhead coefficient for  $i^{\text{th}}$  gate, and  $N$  is the number of the gates in the quantum circuit. Suppose the error  $\varepsilon_i$  for each gate is small, the cost  $C_i$  is close to 1. A first order expansion gives  $C_i \approx 1 + \lambda_i \varepsilon_i$  and thus the total overhead  $C_N$  is approximated as

$$C_N \approx \prod_i (1 + \lambda_i \varepsilon_i). \quad (19)$$

For simplicity, we assume  $\lambda_i = \lambda$  and  $\varepsilon_i = \varepsilon$  are independent of  $i$ . Then we have

$$C_N \approx (1 + \lambda\varepsilon)^N = (1 + \lambda\varepsilon)^{\frac{1}{\lambda\varepsilon} \lambda\varepsilon N} \approx e^{\lambda\varepsilon N} = e^{\lambda\varepsilon_N}. \quad (20)$$

Here we denote  $\varepsilon_N = \varepsilon N$  to be the total error rate of all the  $N$  gates. Then it is not hard to see that the total cost  $C_N$  increase exponentially to the total error rate  $\varepsilon_N$ . However, with a constant total error rate  $\varepsilon_N$ , we still have a constant overhead. Thus a constant total error rate is generally the assumption for error mitigation for digital quantum computing.

## STOCHASTIC ERROR MITIGATION

As discussed in the above section, the QEM method assumes the noise appears either before or after each gate in a digital gate-based quantum computer, but realistic noise occurring in the experimental apparatus is more complicated. Specifically, every gate in digital circuits or every process in analog simulation is physically realised via a continuous real time evolution of a Hamiltonian and thus errors can either inherently mix with the evolution making it strongly gate or process dependent, or act on multiple number of qubits leading to highly nonlocal correlated effects (crosstalks). Since conventional quantum error mitigation methods are restricted to gate-based digital quantum computers and over-simplified noise models, they fail to work for realistic errors and general continuous quantum processes. In this section, we extend the QEM method to a more practical scenario and show how to mitigate errors for these inherent dynamics-based and nonlocal noise in practical noisy quantum devices.

### Pauli transfer matrix representation

We first introduce the Pauli transfer matrix representation of states, observables, and channels as a preliminary. By using Pauli transfer representation, a state and an observable are mapped to a real column and row vectors respectively, as follows

$$\begin{aligned} |\rho\rangle\rangle &= [\dots \rho_k \dots] \\ \rho_k &= \text{Tr}(P_k \rho), \end{aligned} \quad (21)$$

and

$$\begin{aligned} \langle\langle Q| &= [\dots Q_k \dots] \\ Q_k &= \frac{1}{d} \text{Tr}(Q P_k), \end{aligned} \quad (22)$$

where  $P_k \in \{I, \sigma_x, \sigma_y, \sigma_z\}^{\otimes n}$ ,  $n$  is the number of qubits, and  $d = 2^n$ . Furthermore, for a process, i.e.,  $\mathcal{E}(\rho) = \sum_k K_k \rho K_k^\dagger$ , the Pauli transfer matrix representation can be expressed as

$$E_{k,j} = \frac{1}{d} \text{Tr}(P_k \mathcal{E}(P_j)). \quad (23)$$

By using the Pauli transfer representation, we have

$$\text{Tr}(Q \mathcal{E}(\rho)) = \langle\langle Q| E |\rho\rangle\rangle. \quad (24)$$

### Continuous error mitigation scheme

We first illustrate the detailed procedure of continuous error mitigation. We can rewrite the evolution of noisy and ideal quantum states by using infinitesimal  $\delta t$  as

$$\begin{aligned} \rho_N(t + \delta t) &= \rho_N(t) + \delta t \{ -i[H(t), \rho_N(t)] + \lambda \mathcal{L}[\rho_N(t)] \} \\ \rho_I(t + \delta t) &= \rho_I(t) + \delta t \{ -i[H(t), \rho_I(t)] \}, \end{aligned} \quad (25)$$

where  $H(t)$  denotes the ideal Hamiltonian with  $\mathcal{L}$  corresponding to the noisy evolution. In the presence of Markovian stochastic noise involved with environment,

$$\mathcal{L}[\rho] = \sum_k (2L_k \rho L_k^\dagger - L_k^\dagger L_k \rho - \rho L_k^\dagger L_k), \quad (26)$$

while the dynamics induced with the undesired Hamiltonian  $H_C(t)$  which causes coherent errors can be described as

$$\mathcal{L}[\rho] = -i[H_C(t), \rho]. \quad (27)$$

The latter case occurs due to the imperfection of the analog quantum simulators and implementation of quantum logic gates from physical Hamiltonians [30, 60]. For systems with finite-range interactions, Bairey *et al* and Silva *et al* proposed methods that uses only local measurements to reconstruct local Markovian dynamical process [85, 86]. We will show how to eliminate these errors by using continuous error mitigation method.

By using the Pauli transfer matrix representation, Eq. (25) is mapped to  $|\rho_\alpha(t + \delta t)\rangle\rangle = (I + E_\alpha(t)\delta t) |\rho_\alpha(t)\rangle\rangle$  where  $|\rho_\alpha(t)\rangle\rangle$  ( $\alpha = N, I$ ) is the vectorised density matrix of  $\rho_\alpha(t)$  and  $E_\alpha(t)$  corresponds to the second term of Eqs. (25). Equivalently, the superoperator representation of the evolution gives  $\rho_\alpha(t + \delta t) = \mathcal{E}_\alpha(t)\rho_\alpha(t)$ . In the following, we will use these two equivalent representations interchangeably. Note that the evolution induced by  $\mathcal{E}_\alpha$  in the main text becomes  $I + E_\alpha\delta t$  in the Pauli transfer representation. We introduce the recovery operation  $I + E_Q\delta t$  to obtain the ideal dynamics, which can be expressed as

$$(I + E_Q\delta t)(I + E_N\delta t) = I + E_I\delta t + \mathcal{O}(\delta t^2) \quad (28)$$

such that  $E_Q = E_I - E_N$ . Note that  $(I + E_Q\delta t)$  corresponds to  $\mathcal{E}_Q$  in the main text. Due to the linearity of the representation, we can see that  $E_Q$  corresponds to the Pauli transfer matrix representation of  $-\lambda \mathcal{L}[\rho_N(t)]$ . In this framework,  $\mathcal{E}_I(t) \approx \mathcal{E}_N(t)$  holds within a sufficiently small time step  $\delta t$ .

The experimental errors including the interactions with the open environment, undesired couplings and imperfections in the quantum simulators are generally local and we therefore assume  $\mathcal{E}_Q$  can be decomposed into local operators as  $\mathcal{E}_Q = \sum_{S=1}^{N_S} \mathcal{E}_Q^{(S)}$ , where  $\mathcal{E}_Q^{(S)}$  operates on polynomial subsystems of the  $N$ -qubit quantum system. We now decompose the operation  $\mathcal{E}_Q$  into the set of basis operations as

$$\mathcal{E}_Q^{(S)} = \sum_{j \geq 0} q_j^{(S)} \mathcal{B}_j^{(S)}, \quad (29)$$

where  $q_j^{(S)}$  is the quasi-probability and  $\mathcal{B}_j^{(S)}$  is the basis operation for compensating the errors. Note that  $\mathcal{B}_j^{(S)}$  only acts on the same small subsystem as  $\mathcal{E}_Q^{(S)}$ . By performing basis operations for  $\mathcal{E}_Q^{(S)}$  with corresponding quasi-probability distributions in Eq. (29), we can implement the overall quasi-probability operations corresponding to  $\mathcal{E}_Q$  as shown below. Therefore, we can extend the quasi-probability operations into a large-scale system. We remark that this quasi-probability approach works for any errors and we can mitigate correlated stochastic noise and unwanted interactions between (a small number of) multiple qubits. In addition, this argument can be naturally applied to multi-level systems when we can prepare basis operations for them.

In particular, the quasi-probability operation at time  $t$  takes the form of

$$\begin{aligned} \mathcal{E}_Q &= (1 + q_0 \delta t) \mathcal{I} + \sum_{i \geq 1} q_i \delta t \mathcal{B}_i, \\ &= c \left( p_0 \mathcal{I} + \sum_{i \geq 1} \alpha_i p_i \mathcal{B}_i \right) \end{aligned} \quad (30)$$

where  $\mathcal{B}_0$  is set to be an identity operation and we also omit the superscript  $(S)$  for simplicity. The probability to generate the identity operation  $\mathcal{I}$  and  $\mathcal{B}_i$  ( $i \geq 1$ ) is  $p_0 = 1 - \sum_{i \geq 1} p_i$  and  $p_i = |q_i| \delta t / c$  ( $i \geq 1$ ), where  $c = \sum_{i \geq 0} p_i = 1 + (q_0 + \sum_{i \geq 1} |q_i|) \delta t$ . In addition, the parity  $\alpha_0$  for  $\mathcal{B}_0 = \mathcal{I}$  is always unity, and the parity  $\alpha_i$  corresponding to  $\mathcal{B}_i$  ( $i \geq 1$ ) equals to  $\text{sign}(q_i)$ .

The overhead coefficient  $c$  corresponding to  $\mathcal{E}_Q^{(S)}$  is given by  $c = 1 + C_1^{(S)} \delta t$ , with  $C_1^{(S)} := (q_0 + \sum_{i \geq 1} |q_i|)$ . As we have discussed above, this coefficient introduces a sampling overhead. The overhead coefficient from  $t = 0$  to  $t = T$  within infinitely small discretisation  $\delta t$  is

$$C(T) = \lim_{\delta t \rightarrow 0} \prod_S \prod_{k=0}^{T/\delta t} (1 + C_1^{(S)} \delta t) = \prod_S \exp(C_1^{(S)} T). \quad (31)$$

Note that  $|q_i| \propto \lambda$ , therefore we have  $C_1 \propto \lambda$ , and the overall overhead is

$$C(T) = \exp(O(\lambda T)). \quad (32)$$

Here we choose a proper normalisation  $\lambda$  so that the contribution of  $\mathcal{L}$  is bounded by a constant  $l$ :  $\|\mathcal{L}_{\text{exp}}\|_1 \leq l$ . Here, we define the super-operator norm by  $\|\Phi\|_1 = \sup_A \{\|\Phi(A)\|_1 / \|A\|_1 : A \neq 0\}$  with  $\|A\|_1 = \text{Tr}|A|$ . Therefore, given a finite number of samples in the experiments the condition that the scheme works efficiently with a constant resource cost is  $\lambda T = O(1)$ . By interpreting  $\lambda T$  as the total noise strength, the requirement is thus consistent with the case of DQS.

It is also possible to consider time-dependent recovery operation for suppressing time-dependent noise. In this case, the quasi-probability becomes time-dependent and can be obtained by Eq. (29). Therefore, the overall overhead for time-dependent noise is

$$C(T) = \lim_{\delta t \rightarrow 0} \prod_S \prod_{k=0}^{T/\delta t} (1 + C_1^{(S)}(k \delta t) \delta t) = \prod_S \exp \left( \int_0^T C_1^{(S)}(t) dt \right). \quad (33)$$

### Comparison with conventional error mitigation

Errors, occurring in the continuous time evolution, can inherently mix and propagate with the evolution leading to highly nonlocal correlated effects. For instance, dominant errors in superconducting qubits are inherent system

dephasing or relaxation, and coherent errors (or crosstalk) when applying entangling gates. Analog quantum simulators may not even implement discretised quantum gates. Therefore, conventional quantum error mitigation methods fail to work for realistic errors and general continuous quantum processes. Our work addresses the problems by first considering a more general scenario of a continuous process with realistic noise models. More concretely, we consider the time-independent Lindblad master equation

$$\frac{d\rho}{dt} = (\mathcal{H} + \mathcal{L})(\rho) \quad (34)$$

with dynamics of Hamiltonian (including coherent errors) and incoherent Markovian process

$$\begin{aligned} \mathcal{H}(\rho) &= -i[H + \delta H, \rho] \\ \mathcal{L}(\rho) &= \sum_k (2L_k \rho L_k^\dagger - L_k^\dagger L_k \rho - \rho L_k^\dagger L_k), \end{aligned} \quad (35)$$

which describes either gate synthesis in digital quantum computing or the continuous evolution of a analog quantum simulator. Here  $\delta H$  and  $\mathcal{L}$  describe coherent errors (such as crosstalk or imperfections of Hamiltonian) and inherent coupling with the environment (such as dephasing and damping), respectively. We note that even though the coherent error  $\delta H$  and the Lindblad operators  $L_k$  act locally on the quantum system, the effect of errors propagates to the entire system after the evolution. Therefore, such global effects of noise cannot be effectively mitigated using the conventional quasi-probability method, which assumes simple gate-independent error model described by single- or two-qubit error channels before or after each gate.

Our work proposes two key techniques to overcome this problem.

1. First, we discretise the continuous time into small time steps so that we sequentially apply error mitigation for the noisy evolution at each time step. We emphasise that discretised evolution is yet not equivalent to discretised digital computing with local single and two qubit gates. This is because the continuous evolution even with a small time step could be a joint evolution (effectively a joint quantum gate) on all the qubits. Therefore, we directly mitigate errors of all the evolved qubits in each small time evolution, whereas conventional error mitigation methods operate on each local gate. This also explains why we can mitigate crosstalk of multiple qubits, whereas conventional methods only mitigate the effective noise channel for each gate. In practice, one can choose a sufficiently small time step so that the error mitigation works in a 'continuous' way.
2. However, continuous error mitigation with small discretised time requires to constantly pause the original evolution to apply recovery operations and the time discretisation also introduces additional errors. To resolve these problems, we further introduce stochastic error mitigation, which equivalently simulates the continuous error mitigation procedure with infinitely small time step. The stochastic error mitigation method thus simultaneously solves all the issues and provides our final solution for error mitigation of a continuous process. We note that stochastic error mitigation only requires to apply a small number of single-qubit recovery operations at certain times. We can thus pre-engineer the recovery operations into the original evolution Hamiltonian without interrupting the simulation.

To summarise, the first contribution of our work is to solve a major open problem of mitigating realistic (inherently gate- or process-mixed and nonlocal) noise for both digital and analog quantum simulators, which has strong applications in achieving quantum advantage with near-term noisy quantum devices. The techniques we introduce for the stochastic error mitigation method are highly non-trivial and do represent significant advances in our understanding of mitigating multi-qubit errors for processes beyond discretised gates and over-simplified noise models.

## Decomposition of the recovery operation and optimisation

### *Complete basis operation set*

In Ref [5], it is shown that every single qubit operation can be emulated by using 16 basis operations. This is because every single qubit operation (including projective measurements) can be expressed with square matrices with  $4 \times 4 = 16$  elements by using the Pauli transfer representation [91]. Therefore, 16 linearly independent operations are sufficient to emulate arbitrary single qubit operations. In Table I, we show one efficient set of basis operations for a single qubit in Ref [5].

1	$[I]$ (no operation)	2	$[\sigma^x]$	3	$[\sigma^y]$	4	$[\sigma^z]$
5	$[R_x] = [\frac{1}{\sqrt{2}}(I + i\sigma^x)]$	6	$[R_y] = [\frac{1}{\sqrt{2}}(I + i\sigma^y)]$	7	$[R_z] = [\frac{1}{\sqrt{2}}(I + i\sigma^z)]$	8	$[R_{yz}] = [\frac{1}{\sqrt{2}}(\sigma^y + \sigma^z)]$
9	$[R_{zx}] = [\frac{1}{\sqrt{2}}(\sigma^z + \sigma^x)]$	10	$[R_{xy}] = [\frac{1}{\sqrt{2}}(\sigma^x + \sigma^y)]$	11	$[\pi_x] = [\frac{1}{2}(I + \sigma^x)]$	12	$[\pi_y] = [\frac{1}{2}(I + \sigma^y)]$
13	$[\pi_z] = [\frac{1}{2}(I + \sigma^z)]$	14	$[\pi_{yz}] = [\frac{1}{2}(\sigma^y + i\sigma^z)]$	15	$[\pi_{zx}] = [\frac{1}{2}(\sigma^z + i\sigma^x)]$	16	$[\pi_{xy}] = [\frac{1}{2}(\sigma^x + i\sigma^y)]$

TABLE I. Sixteen basis operations. These operations are composed of single qubit rotations and measurements.  $[I]$  denotes an identity operation (no operation),  $[\sigma^i]$  ( $i = x, y, z$ ) corresponds to operations applying Pauli matrices.  $[\pi]$  corresponds to projective measurements.

Here, we denote the complete basis operations as  $\{\mathcal{B}_i\}$ . For multiple qubit systems, tensor products of single qubit operations, e.g.,  $\mathcal{B}_i \otimes \mathcal{B}_j$  also forms a complete basis set for composite systems. Therefore, if we can implement the complete basis operations for a single qubit, we can also emulate arbitrary operations for multiple qubits systems.

By using only observables within spatial domain, we can recover the Lindbladian acting on this domain and reconstruct the local Markovian dynamics [85]. Here, we provide the recovery operations for several typical Markovian processes during the quantum simulation. The recovery operations can be analytically expressed as  $\mathcal{E}_Q = \mathcal{I} - \lambda \mathcal{L} \delta t$ . For depolarising, dephasing and amplitude damping, the recovery operations  $\mathcal{E}_Q$  can be decomposed as

$$\begin{aligned}
\mathcal{E}_Q^{\text{depolarise}} &= (1 + \frac{3}{4}\lambda\delta t)\mathcal{I} - \frac{\lambda}{4}(\mathcal{X} + \mathcal{Y} + \mathcal{Z})\delta t \\
\mathcal{E}_Q^{\text{dephase}} &= (1 + \lambda\delta t)\mathcal{I} - \lambda\mathcal{Z}\delta t \\
\mathcal{E}_Q^{\text{amp}} &= (1 + \frac{1}{4}\lambda\delta t)\mathcal{I} + \lambda(-\frac{1}{2}\mathcal{X} - \frac{1}{2}\mathcal{Y} - \frac{1}{4}\mathcal{Z} + [R_{xy}] + [\pi_{xy}])\delta t
\end{aligned} \tag{36}$$

respectively.

#### Optimising the resource cost by linear programming

Over-complete basis can be used to further reduce the resource cost for the stochastic error mitigation scheme. In general, the target quasi-probability operation  $E_Q$  can be decomposed as a linear combination of unitary channels and projective measurements by using Pauli transfer matrix representation. The quasi-probability operation  $\mathcal{E}_Q$  can be decomposed into a complete basis  $\{\mathcal{B}_i\}$  as

$$E_Q = \sum_i q_i B_i, \tag{37}$$

where we set  $B_0 = I$ . Given the target quasi-probability operation  $E_Q$ , the overall resource cost for quasi-probability scheme is given by  $C(T) = \exp(C_1 T)$  with  $C_1 = q_0 + \sum_{i \geq 1} |q_i|$ .

In order to minimise the resource cost, we aim to reduce  $C_1$ . Consider an over-complete basis  $\{B'_i\}$  which includes the complete basis  $\{B_i\}$  and also other randomly generated unitary operators and projective measurements. Then the quasi-probability operation  $E_Q$  is decomposed into this over-complete basis  $\{B'_i\}$  as

$$E_Q = \sum_i q'_i B'_i. \tag{38}$$

Minimising  $C_1 = q_0 + \sum_{i \geq 1} |q_i|$  can be further rewritten as a linear programming as follows,

$$\begin{aligned}
\min C_1 &= q_0 + \sum_{i \geq 1} (q_i^+ - q_i^-), \\
s.t. \quad E_Q &= \sum_i (q_i^+ - q_i^-) B'_i, \\
q_i^+, q_i^- &\geq 0.
\end{aligned} \tag{39}$$

The overall resource cost  $C(T)$  for stochastic error mitigation scheme can therefore be reduced by this optimisation method.

### Equivalence between continuous error mitigation and stochastic error mitigation

Since the continuous error mitigation scheme requires to apply instant recovery operation at each time  $t$ , it also makes its realisation challenge in practice. Note that the recovery operation is,

$$\mathcal{E}_Q = c \left( p_0 \mathcal{I} + \sum_{i \geq 1} \alpha_i \tilde{p}_i \delta t \mathcal{B}_i \right), \quad (40)$$

with  $p_0 = 1 - \mathcal{O}(\delta t)$  and  $\tilde{p}_i = p_i / \delta t = \mathcal{O}(1)$ . We can interpret it as with probability  $1 - \sum_i \tilde{p}_i \delta t$  we do nothing, and with probability  $\tilde{p}_i \delta t$  we apply a corresponding correction operation. We also multiply  $c \cdot \alpha_i$  to the output measurement. We can regard the event that applies the correction operations as a jump similar to the stochastic Schrödinger equation approach.

Starting at time  $t = 0$ , the probability that there is no jump until time  $t$  is

$$Q(t) = \lim_{\delta t \rightarrow 0} \prod_{i=0}^{t/\delta t} \left( 1 - \sum_{i \geq 1} \tilde{p}_i \delta t \right) = e^{-\int_0^t \Gamma(t') dt'} \quad (41)$$

where  $\Gamma(t) = \sum_{i \geq 1} \tilde{p}_i(t)$ . The probability to have jump in the time interval  $[t, t + dt]$  is

$$P(t)dt = \Gamma(t) e^{-\int_0^t \Gamma(t') dt'} dt. \quad (42)$$

Now suppose we generate a uniformly distributed random variable  $q \in [0, 1]$  and solve

$$q = e^{-\int_0^{t_{\text{jp}}} \Gamma(t') dt'}, \quad (43)$$

to determine the jump time  $t_{\text{jp}}$ . Then the probability that jump happens at time  $t_{\text{jp}}$  or in particular between  $[t_{\text{jp}}, t_{\text{jp}} + dt]$  is

$$dq = P(t)dt, \quad (44)$$

which agrees with Eq. (42). We can thus use the uniformly distributed random variable  $q$  to determine the jump time to equivalently simulate the original continuous error mitigation process.

Now, at the jump time  $t_{\text{jp}}$ , we apply the basis operation other than the identity operation. We can determine the basis operation by generating another uniformly distributed random number  $q' \in [0, 1]$ . If  $q' \in [s_{k-1}, s_k]$ , we set the basis operation to  $\mathcal{B}_k$ , where  $s_k(t) = (\sum_{j=1}^k \tilde{p}_j) / (\sum_{j=1}^{N_{\text{op}}} \tilde{p}_j)$  and  $N_{\text{op}}$  is the number of the basis operations.

We can pre-determine the jump time  $t_{\text{jp}}^1, t_{\text{jp}}^2, \dots, t_{\text{jp}}^k$  from Eq. (43). For time-independent noise, the jump time can be simply determined as  $t_{\text{jp}} = \log(q) / \sum_{i \geq 1} \tilde{p}_i$  with  $q$  randomly generated from  $[0, 1]$ . Given evolution time  $T$ , the average number of recovery operations is proportional to  $\mathcal{O}(\lambda T)$ . In the numerics, the average number of recovery operations is about 0.3 times per evolution on average.

### Implementation of the error-mitigated quantum simulation

Analog quantum simulators can more efficiently and robustly simulate specific systems, enabling the possibility of probing classically intractable many-body phenomena with NISQ devices. In experiment, analog quantum simulation (AQS) has been applied for studying non-equilibrium dynamics, quantum scrambling, Ising and Bose-Hubbard models, dynamical quantum phase transitions, etc. Among different proposals for quantum computing, analog quantum simulators directly realise the continuous time evolution for the whole system and hence our QEM method can be directly used for AQS. In the section, we show how to implement the error-mitigated analog quantum simulation in more details.

As shown in Fig. 5, our work considers an intermediate scenario between AQS and DQS. Compared to a fully AQS, we insert a constant number  $\mathcal{O}(\lambda T)$  of single qubit operations in the whole evolution of Hamiltonian simulation. The joint evolution and the single qubit dynamics can be pre-engineered by using Algorithm 1, which can be regarded as a modified evolution of AQS. Compared to a fully DQS, our simulator does not need to synthesise each gate and there is no two-qubit gate and hence significantly avoid less crosstalks. Since our scenario only additionally requires single

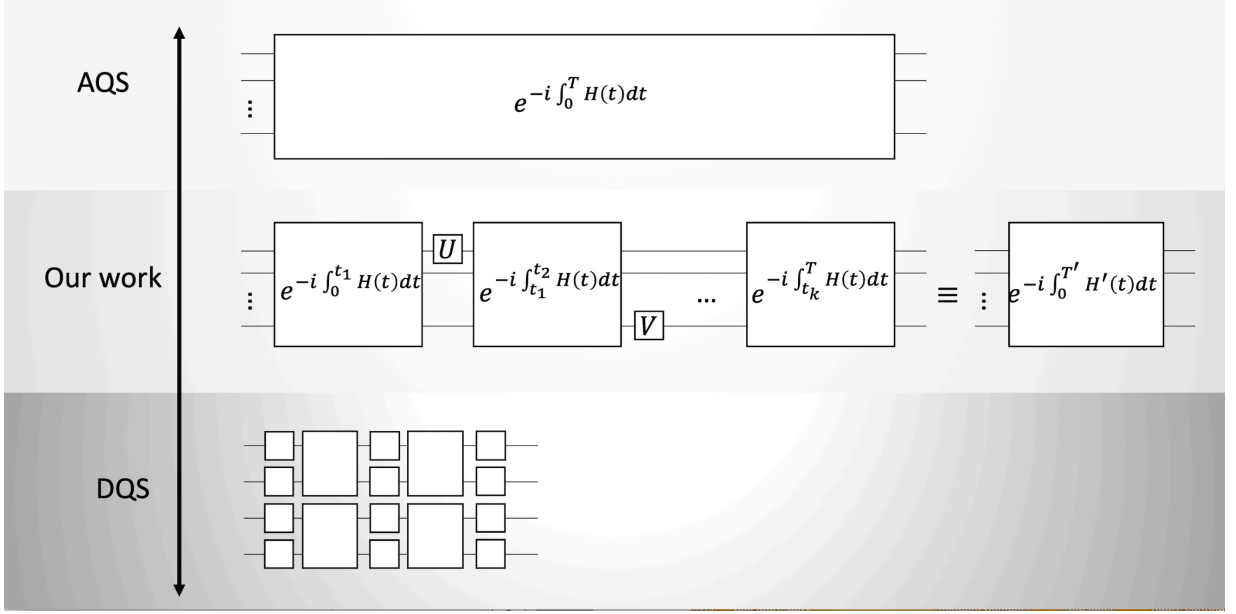


FIG. 5. Comparison between analog quantum simulator (AQS), the scenario considered in our work, and digital quantum simulator (DQS). AQS directly implements the joint dynamics of all qubits. Our work considers joint dynamics of all qubits sandwiched with single qubit dynamics to mitigate the errors accumulated in the evolution.

qubit operations that are meanwhile allowed in practice, we categorise it to AQS. However, one may also regard it as a modified analog-digital quantum simulation, where we directly apply joint plus local gates (evolution) on every qubit. This analog-digital quantum simulation [81] has been experimentally implemented with superconducting circuits for Dicke model and fermion-fermion scattering in the context of quantum field theories [69, 70] and with trapped ions for open system simulation [92]. Therefore, our scheme can be implemented on the current digital quantum simulators or analog quantum simulators.

As the evolution of most quantum simulators are based on external pulses, such as trapped ions and superconducting qubits, it would be practically feasible to interrupt the continuous evolution by simply turning off the external pulses and then turning on the single qubit recovery pulses. Alternatively, we can also apply single qubit recovery pulses with short duration and sufficiently strong intensity compared to the parameters of the AQS Hamiltonian so that error mitigation procedure does not induce additional errors. Furthermore, since the recovery operations are pre-determined, one can simply pre-engineer the single qubit dynamics into the joint evolution so that it is basically equivalent to an AQS with time-dependent Hamiltonians, as shown in Fig. 5. While the recovery operation mitigates errors during the continuous evolution, errors during the recovery operation can be mitigated via the hybrid approach, which we will discuss in the section .

## HYBRID ERROR MITIGATION

In this section, we show how to apply the extrapolation method to mitigate model estimation error and the errors associated with imperfect recovery operations. Combined with stochastic error mitigation, we thus propose a hybrid error mitigation method for errors in practical NISQ devices.

### Boosting model estimation error

We first show how to boost model estimation error, which will be used for its mitigation. Assume that the evolution of the quantum system is described by the open-system master equation

$$\frac{d}{dt}\rho_\lambda = -i[H(t), \rho_\lambda] + \lambda \mathcal{L}_{\text{exp}}[\rho_\lambda]. \quad (45)$$



The evolution of the system under a scaled Hamiltonian drive  $\frac{1}{r}H\left(\frac{t}{r}\right)$  takes the form of

$$\frac{d}{dt}\rho'_\lambda = -i\left[\frac{1}{r}H\left(\frac{t}{r}\right), \rho'_\lambda\right] + \lambda\mathcal{L}_{\text{exp}}[\rho'_\lambda]. \quad (46)$$

Assuming the noise superoperator  $\mathcal{L}$  is invariant under rescaling, we have

$$\begin{aligned} \frac{d}{dt}\rho'_\lambda(rt) &= \frac{dt'}{dt} \frac{\partial}{\partial t'} \rho'_\lambda(t') \Big|_{t'=rt} \\ &= r \left\{ -i \left[ \frac{1}{r} H\left(\frac{t'}{r}\right), \rho'_\lambda(t') \right] + \lambda \mathcal{L}[\rho'_\lambda(t')] \right\} \Big|_{t'=rt} \\ &= -i[H(t), \rho'_\lambda(rt)] + r\lambda\mathcal{L}[\rho'_\lambda(rt)]. \end{aligned} \quad (47)$$

On the other hand, the density matrix  $\rho_{r\lambda}(t)$  with enhanced noise strength  $r\lambda$  is given by

$$\frac{d}{dt}\rho_{r\lambda}(t) = -i[H(t), \rho_{r\lambda}(t)] + r\lambda\mathcal{L}[\rho_{r\lambda}(t)]. \quad (48)$$

Comparing Eqs. (47) and (48), one finds that  $\rho'_\lambda(rt)$  and  $\rho_{r\lambda}(t)$  follow the same differential equation, and thus with the initial conditions  $\rho'_\lambda(0) = \rho_{r\lambda}(0)$  we prove  $\rho'_\lambda(rt) = \rho_{r\lambda}(t)$ . This indicates by evolving the re-scaled Hamiltonian for time  $rt$ , we can effectively boost physical errors of quantum systems.

Now, we discuss how to boost the model estimation error. By applying stochastic error mitigation, we obtain

$$\frac{d}{dt}\rho_\lambda^{(Q)}(t) = -i[H(t), \rho_\lambda^{(Q)}(t)] + \lambda\Delta\mathcal{L}[\rho_\lambda^{(Q)}(t)], \quad (49)$$

where  $\rho_\lambda^{(Q)}(t)$  is the error mitigated effective density matrix after stochastic error mitigation. Assuming  $\Delta\mathcal{L} = \mathcal{L}_{\text{exp}} - \mathcal{L}_{\text{est}}$  is invariant under re-scaling of the Hamiltonian, we can similarly obtain

$$\frac{d}{dt}\rho_{r\lambda}^{(Q)}(t) = -i[H(t), \rho_{r\lambda}^{(Q)}(t)] + r\lambda\Delta\mathcal{L}[\rho_{r\lambda}^{(Q)}(t)]. \quad (50)$$

This can be experimentally achieved by applying stochastic error mitigation for a re-scaled time  $rt$  under the re-scaled Hamiltonian.

It is worth noting that even if the noise model is time dependent, our method can still work as long as the evolution can be described by a Lindblad equation and its dependence on time is known. For example, when we consider a time dependent noisy process with stochastic error mitigation described by

$$\frac{d\rho_\lambda^{(Q)}(t)}{dt} = -i[H(t), \rho_\lambda^{(Q)}(t)] + \lambda t \Delta\mathcal{L}_0[\rho_\lambda^{(Q)}(t)], \quad (51)$$

where  $\Delta\mathcal{L}_0$  is time independent. Then, the re-scaled dynamical equation becomes

$$\frac{d\rho_\lambda'^{(Q)}(rt)}{dt} = -i[H(t), \rho_\lambda'^{(Q)}(rt)] + r^2\lambda t \Delta\mathcal{L}_0[\rho_\lambda'^{(Q)}(rt)]. \quad (52)$$

In this case, we can interpret that the noise rate is boosted by a factor of  $r^2$ . We will later show how such a time dependent noise process can be mitigated in Sec. .

### Richardson's extrapolation for physical errors and model estimation errors

In this section, we briefly review the extrapolation method proposed in Ref. [3, 4]. We assume the open system evolution is described by

$$\frac{d\rho_N(t)}{dt} = -i[H_{\text{sim}}(t), \rho_N(t)] + \lambda\mathcal{L}_{\text{exp}}[\rho_N(t)]. \quad (53)$$

In Ref. [4], it is shown that the expectation value of an observable  $O$  can be expressed as

$$\langle O(\lambda) \rangle = \langle O(0) \rangle + \sum_{k=1}^n \alpha_k \lambda^k + B_{n+1}(\lambda, \mathcal{L}, T), \quad (54)$$

where  $\alpha_k \approx O(N^k T^k)$  and  $B_{n+1}(\lambda, \mathcal{L}, T)$  is upper bounded by

$$B_{n+1}(\lambda, \mathcal{L}, T) \leq \|O\| a_{n+1} \frac{\lambda^{n+1} T^{n+1}}{(n+1)!}, \quad (55)$$

where  $\|O\| = \max_{\psi} \langle \psi | O | \psi \rangle$  is the spectra norm of  $O$ . Here, in the case that  $\mathcal{L}$  is a Lindblad type operator, one can have the bound for  $a_{n+1}$  as

$$a_{n+1} \leq \|\mathcal{L}_{\text{exp}}\|_1^{n+1}. \quad (56)$$

Now, we have

$$B_{n+1}(\lambda, \mathcal{L}, T) \leq \|O\| \frac{(\lambda T \|\mathcal{L}_{\text{exp}}\|_1)^{n+1}}{(n+1)!}. \quad (57)$$

In order to employ the extrapolation method, we need to obtain the expectation value of observable  $\langle O(r_j \lambda) \rangle$  ( $j = 0, 1, \dots, n, r_0 = 1$ ) at time  $t = T$  corresponding to the equation

$$\frac{d}{dt} \rho_{\lambda}(t) = -i [H(t), \rho_{\lambda}(t)] + r_j \lambda \mathcal{L}(\rho_{\lambda}(t)), \quad (58)$$

which can be obtained by using the re-scaling of the Hamiltonian as described in section . Then we can obtain the approximation of the noise free expectation value of the observable  $O$  as

$$\langle O(0) \rangle_n^* = \sum_{j=0}^n \beta_j \langle O \rangle'_{r_j \lambda}, \quad (59)$$

where  $\langle O(0) \rangle_n^*$  is the estimated noise free expectation value up to an error of order  $O(\lambda^{n+1})$ , and  $\langle O \rangle'_{r_j \lambda}$  are the measurement outcome corresponding to the state  $\rho_{r\lambda}(T)$ . Here the coefficients  $\beta_j = \prod_{l \neq j} r_l (r_l - r_j)^{-1}$  are defined by the solution of the following equations

$$\sum_{j=0}^n \beta_j = 1, \quad \sum_{j=0}^n \beta_j r_j^k = 0, \quad k = 1, \dots, n. \quad (60)$$

In Ref. [4], it has been shown that the difference between the estimator and the error free expectation value is bounded by

$$|\langle O(0) \rangle_n^* - \langle O \rangle_I| \leq \gamma_n \left( \frac{r_{\max}^{n+1} \Delta_{\max}}{\sqrt{N_{\text{sample}}}} + \|O\| \frac{(r_{\max} \lambda T \|\mathcal{L}_{\text{exp}}\|_1)^{n+1}}{(n+1)!} \right), \quad (61)$$

where  $\gamma_n = \sum_{j=0}^n |\beta_j|$ ,  $r_{\max} = \max_j r_j$ , and  $\Delta_{\max}/\sqrt{N_{\text{sample}}}$  is the largest experimental errors due to shot noises with  $N_{\text{sample}}$  being the number of samples. From Eq. (61), we can see that extrapolation methods requires

$$r_{\max} \lambda T \|\mathcal{L}_{\text{exp}}\|_1 = \mathcal{O}(1). \quad (62)$$

Now, under the stochastic error mitigation for a continuous process, Eq. (53) is modified to

$$\frac{d}{dt} \rho_{\lambda}^{(Q)}(t) = -i [H(t), \rho_{\lambda}^{(Q)}(t)] + \lambda \Delta \mathcal{L}[\rho_{\lambda}^{(Q)}(t)], \quad (63)$$

where  $\Delta \mathcal{L} = \mathcal{L}_{\text{exp}} - \mathcal{L}_{\text{est}}$ . Similar to the mitigation of physical errors via Richardson's extrapolation, we can obtain the approximation of the noise free expectation value of the observable  $O$  as

$$\langle O(0) \rangle_n^* = \sum_{j=0}^n \beta_j \langle O \rangle_{r_j \lambda}, \quad (64)$$

where  $\langle O(0) \rangle_n^*$  is the estimated noise free expectation value up to an error of order  $O(\lambda^{n+1})$ , and  $\langle O \rangle_{r\lambda}$  is the measurement outcome after stochastic error mitigation, corresponding to  $\rho_{r\lambda}^{(Q)}(T)$ .

Hence, under stochastic error mitigation, the inequality of (61) is modified to

$$|\langle O(0) \rangle_n^* - \langle O \rangle_I| \leq \gamma_n \left( \frac{C(r_{\max} T) r_{\max}^{n+1} \Delta_{\max}}{\sqrt{N_{\text{sample}}}} + \|O\| \frac{(r_{\max} \lambda T \|\Delta \mathcal{L}\|_1)^{n+1}}{(n+1)!} \right), \quad (65)$$

with Eq. (62) changed into

$$r_{\max} \lambda T \|\Delta \mathcal{L}\|_1 = \mathcal{O}(1). \quad (66)$$

Here, we used the fact that the variance of the error-mitigated expectation value of the observable is amplified with the overhead coefficient  $C$ .

From Eq.(65), the deviation between the ideal measurement outcome and the error-mitigated one is bounded independently with the Hamiltonian, i.e., the to-be-simulated problem. The bound only relies on the noise model, the evolution time, the number of samples, and the parameters used in extrapolation.

## NUMERICAL SIMULATION

As we show in the section , the variation of the performance of our error mitigation methods in terms of different Hamiltonians and noise models is theoretically well bounded, which indicates that the theory does apply for general Hamiltonian simulation with NISQ devices. In this section, we report additional numerical simulation for the transverse field Ising model and frustrated spin-half model as  $J_1 - J_2$  model to verify the viability of our theory.

We first consider a four-qubit 1D transverse field Ising model

$$H = J \sum_{i=1}^4 \sigma_z^{(i)} \sigma_z^{(i+1)} + h \sum_{j=1}^4 \sigma_x^{(j)}. \quad (67)$$

We consider the quantum critical point at  $J = h = 2\pi \times 4$  MHz where correlations exhibits power law decay instead of exponential decay. The noise strength  $\lambda_1 = \lambda_2 = 0.04$  MHz and errors of single-qubit operation  $p_x = p_y = 0.25\%$  and  $p_z = 0.5\%$ , which are the same as in the main text for comparison. We set the initial state to  $(|+\rangle)^{\otimes 4}$  with  $|+\rangle = (|0\rangle + |1\rangle)/\sqrt{2}$ , evolve it to time  $T = 16\pi/J$ , and measure the expectation value of the normalised next-nearest-neighbour correlation function  $\sum_{\langle\langle ij \rangle\rangle} \sigma_x^{(i)} \sigma_x^{(j)}$ . The total number of samples of the measurement is fixed to be  $10^6$ . To demonstrate the performance of stochastic and hybrid error mitigation much clearer, we consider eight-qubit Hamiltonian with infinite number of samples, as shown in Fig. 6(g).

Next, we consider a four-qubit Hamiltonian simulation for  $J_1 - J_2$  frustrated model with field

$$H = J_1 \sum_{\langle ij \rangle} \sigma_z^{(i)} \sigma_z^{(j)} + J_2 \sum_{\langle\langle ij \rangle\rangle} \sigma_z^{(i)} \sigma_z^{(j)} - h \sum_{j=1}^4 \hat{\sigma}_x^{(j)} \quad (68)$$

where  $\langle ij \rangle$  and  $\langle\langle ij \rangle\rangle$  represent nearest-neighbour (NN) and next-nearest-neighbour (NNN) interactions, respectively. This model has been widely investigated to describe the magnetism and phase transitions, and no exact solutions have been found with general values of the coupling constants with general values of the coupling constants  $J_1$  and  $J_2$ . At the point of  $J_2/J_1 = 0.5$ , the ground state of zero-field  $J_1 - J_2$  model is spin dimers and the antiferromagnetic to frustrated phase transition is believed to be near to  $J_2/J_1 \sim 0.5$  [93]. Therefore, a scale-up simulation of these models with error mitigated analog quantum simulators could be applied for discovering new physics. We consider the quantum critical point at  $J_2/J_1 = 0.5$  and set  $J_1 = h = 2\pi \times 2$  MHz in the simulation. We set the initial state to  $(|+\rangle)^{\otimes 4}$ , evolve it to time  $T = 8\pi/J$ , and measure the expectation value of the normalised NN correlation function  $\sum_{\langle ij \rangle} \sigma_x^{(i)} \sigma_x^{(j)}$ . The total number of samples of the measurement and error rates for are set the same as in the main text.

From the simulation results shown in Fig. 6 and 7, we clearly see that our stochastic and hybrid algorithms can effectively suppress the errors during the evolution, which is consistent with the numerical simulation in the main text.

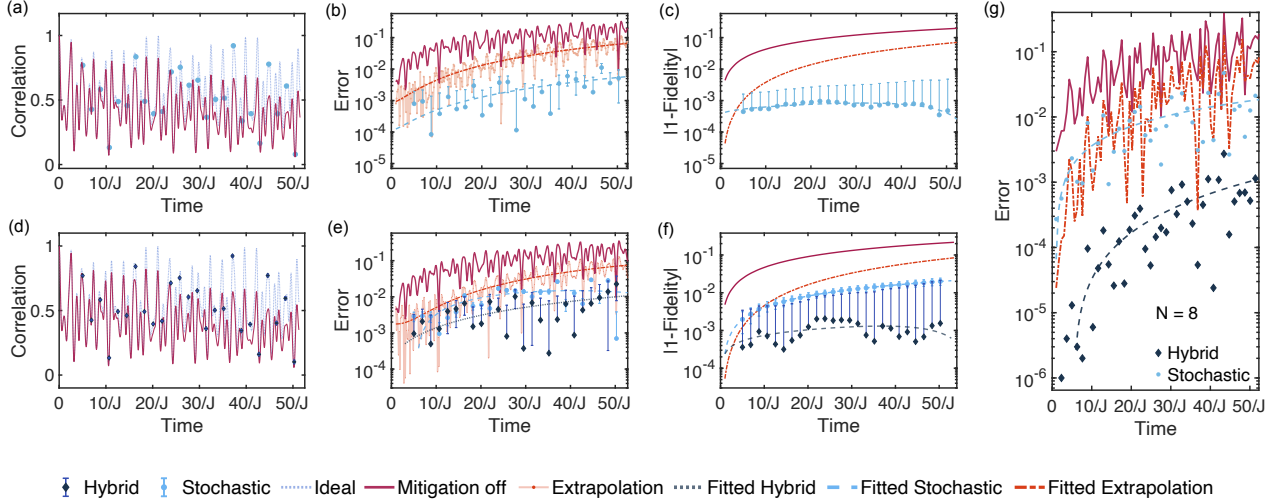


FIG. 6. Numerical test of the performance of error mitigation schemes for transverse field Ising model without model estimation error ((a)(b)(c)) and with 10% model estimation error  $\lambda_{\text{exp}} = 1.1\lambda_{\text{est}}$  ((d)(e)(f)(g)). We consider time evolution of the Ising Hamiltonian with energy relaxation and dephasing. (a)–(f) considers four-qubit Hamiltonian with finite ( $10^6$ ) number of samples. (g) considers eight-qubit Ising spin chain Hamiltonian with infinite number of samples. (a) and (d) compares the time evolved normalised next-nearest-neighbour correlation function. (b) and (e) shows the error between the exact value and the practical value. (c) and (f) shows the fidelity of the effective density matrix  $\rho_{\text{eff}}^\alpha$  and the ideal one  $\rho_I$  under different error mitigation scheme  $\alpha$ . (g) shows that the performance of stochastic and hybrid QEM. Hybrid error mitigation scheme suppresses the error up to about four orders of magnitude even with 10% model estimation error.

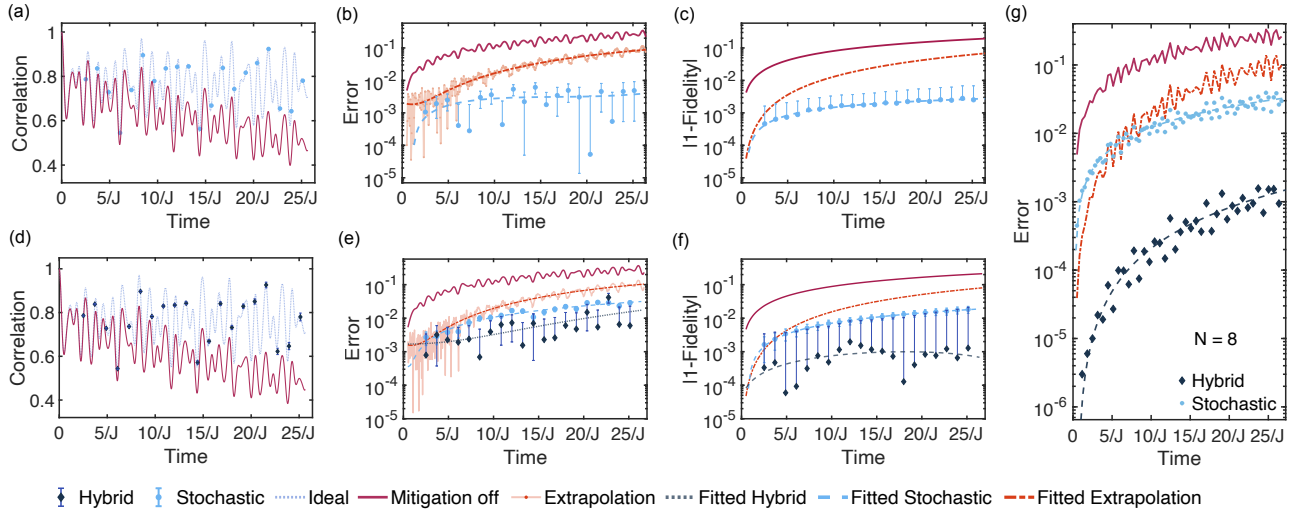


FIG. 7. Numerical test of the performance of error mitigation schemes for frustrated quantum spin model without model estimation error ((a)(b)(c)) and with 10% model estimation error  $\lambda_{\text{exp}} = 1.1\lambda_{\text{est}}$  ((d)(e)(f)(g)). The parameter settings are the same in the main text.

### TIME DEPENDENT NOISE MODEL

Here we show an example that our method also works for time-dependent noise when the time dependence is well characterised. We consider the Ising model under low frequency noise [94–97], which is described by

$$H = \sum_{\langle ij \rangle} J_{ij} \hat{\sigma}_z^{(i)} \hat{\sigma}_z^{(j)} + \sum_{j=1}^n \left( h_j \hat{\sigma}_z^{(j)} + \lambda' f_j(t) \hat{\sigma}_z^{(j)} \right), \quad (69)$$

where  $n$  is the number of qubits,  $\langle ij \rangle$  denotes the interactions between neighbour  $i$  and  $j$ ,  $h_j$  is the coupling of the external magnetic field, and  $f_j(t)$  describes the (noisy) interaction to the environment. We assume that  $f_j(t)$  is a classical Gaussian noise which satisfies  $\overline{f_j(t)} = 0$ ,  $\overline{f_j(t) f_{j'}(t)} = \delta_{jj'}$ , and higher order correlations are zero, where  $\overline{f}$  denotes the ensemble average for a random variable  $f$ . After taking the ensemble average, the evolution of the density matrix averaged over trajectories can be described as

$$\frac{d\overline{\rho(t)}}{dt} \simeq -i[H_0, \rho] + 2\lambda'^2 t \sum_{j=1}^n \left( \hat{\sigma}_z^{(j)} \rho \hat{\sigma}_z^{(j)} - \rho \right), \quad (70)$$

where  $H_0 = \sum_{\langle ij \rangle} J_{ij} \hat{\sigma}_z^{(i)} \hat{\sigma}_z^{(j)} + \sum_{j=1}^n h_j \hat{\sigma}_z^{(j)}$ . We refer a detailed derivation to Sec. .

This result indicates that the averaged trajectory is equivalent to the time-dependent noisy evolution. By applying the hybrid error mitigation method, a combination of stochastic error mitigation and linear extrapolation, we show in Fig. 8 that the time-dependent noise can be mitigated without detailed knowledge of the noise strength and noise type.

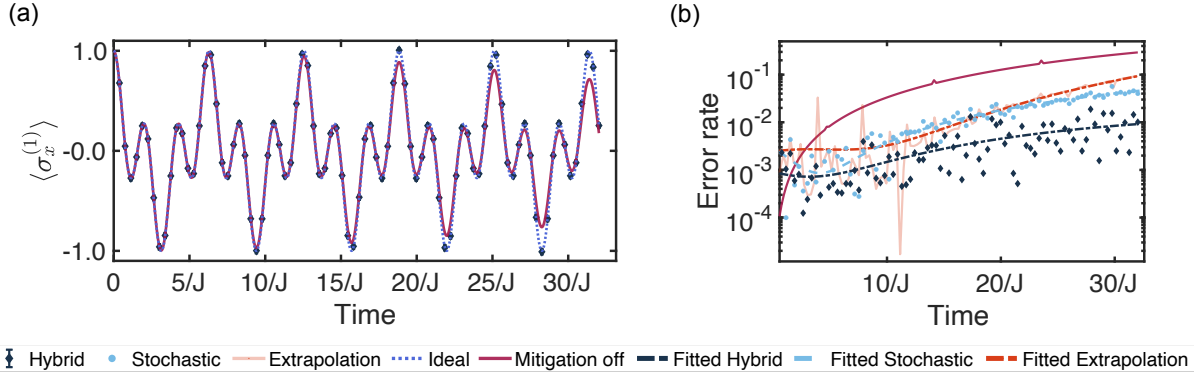


FIG. 8. Numerical test of the performance of error mitigation schemes for a two site quantum system. The system is affected by the time-dependent environmental noise, where the Hamiltonian reads  $H = J \hat{\sigma}_z^{(1)} \hat{\sigma}_z^{(2)} - \sum_{j=1}^2 \left( h_j \hat{\sigma}_z^{(j)} + \lambda' f_j(t) \hat{\sigma}_z^{(j)} \right)$ . We consider a low-frequency noise derived in section , the dynamical equation is expressed as  $\frac{d\overline{\rho(t)}}{dt} \simeq -i[H_0, \rho] + 2\lambda'^2 t \sum_{j=1}^2 \left( \hat{\sigma}_z^{(j)} \rho \hat{\sigma}_z^{(j)} - \rho \right)$ . The time correlated Lindblad noise operator is  $L_{\text{dep}} = \sqrt{t}L$ , where  $L$  has the same form as in Fig. 2. We set the coupling  $J = 2\pi \times 3$  MHz, field strength  $h = 0.5J$ , noise strength  $2\lambda'^2 = 0.1$  MHz, time-dependent model estimation error  $\lambda_{\text{exp}} = 1.2\lambda_{\text{est}}$  and the sampling numbers  $10^5$ . As proven in Eq. (52), noise rate is boosted by a factor  $r_j^2$ , and we used the scaling factor  $r_1 = 1$ ,  $r_2 = 1.5$  for Richardson extrapolation and the hybrid error mitigation.

### Derivation of the time dependent noise model

We consider a generic Ising Hamiltonian with time-dependent environmental noise as

$$H = \sum_{\langle ij \rangle} J_{ij} \hat{\sigma}_z^{(i)} \hat{\sigma}_z^{(j)} + \sum_{j=1}^n \left( h_j \hat{\sigma}_z^{(j)} + \lambda' f_j(t) \hat{\sigma}_z^{(j)} \right), \quad (71)$$

where  $\langle ij \rangle$  denotes the interactions between neighbour  $i$  and  $j$ , and  $f_j(t)$  describes the interaction to the environment.

In the interaction picture, we divide the Schrodinger picture Hamiltonian into two parts:

$$\begin{aligned} H_0 &= \sum_{\langle ij \rangle}^n J_{ij} \hat{\sigma}_z^{(i)} \hat{\sigma}_z^{(j)} + \sum_{j=1}^n h_j \hat{\sigma}_z^{(j)} \\ H_I &= \sum_{j=1}^n \lambda' f_j(t) \hat{\sigma}_z^{(j)}. \end{aligned} \quad (72)$$

The interaction picture is defined through  $\rho_I = e^{iH_0 t} \rho e^{-iH_0 t}$ , and the evolution equation now reads

$$\frac{d\rho_I}{dt} = -i[H_I, \rho_I]. \quad (73)$$

By taking a series expansion, we have

$$\begin{aligned} \rho_I(t) &= \rho_I(0) - i \int_0^t [H(t'), \rho_I] dt' - \int_0^t \int_0^{t'} dt' dt'' [H(t'), [H(t''), \rho_I(t'')]] \\ &\simeq \rho_I(0) - i \int_0^t [H(t'), \rho_I] dt' - \int_0^t \int_0^{t'} dt' dt'' [H(t'), [H(t''), \rho_I(0)]] \end{aligned} \quad (74)$$

By taking an ensemble average of the random variable, we have

$$\overline{\rho_I(t)} \simeq \rho(0) - \lambda'^2 \sum_{j,j'=1}^n \int_0^t \int_0^{t'} dt' dt'' \overline{f_j(t') f_{j'}'(t'')} \left[ \hat{\sigma}_z^{(j)}, \left[ \hat{\sigma}_z^{(j')}, \rho(0) \right] \right] \quad (75)$$

where we have used

$$\overline{f_j(t)} = 0, \overline{f_j(t') f_{j'}(t'')} = \overline{f_j(t' - t'') f(0)}, \overline{f_j(t) f_{j'}(t)} \propto \delta_{j,j'} (j, j' = 1, 2, \dots, n). \quad (76)$$

For the white noise,  $\overline{f_j(t') f_{j'}(t'')} = \tau_c \delta_{t', t''} \delta_{j,j'}$ , Eq. (75) takes the form of

$$\begin{aligned} \overline{\rho_I(t)} &\simeq \rho(0) - \sum_{j=1}^n \lambda'^2 t \tau_c \left( \rho(0) - \hat{\sigma}_z^{(j)} \rho(0) \hat{\sigma}_z^{(j)} \right) \\ &= (1 - \lambda'^2 t \tau_c) \rho(0) + \sum_{j=1}^n \lambda'^2 t \tau_c \hat{\sigma}_z^{(j)} \rho(0) \hat{\sigma}_z^{(j)}. \end{aligned} \quad (77)$$

By taking a small  $t$ , we obtain

$$\frac{d\overline{\rho_I(t)}}{dt} \simeq -\lambda'^2 \frac{\tau_c}{2} \sum_{j=1}^n \left[ \hat{\sigma}_z^{(j)}, \left[ \hat{\sigma}_z^{(j)}, \overline{\rho_I(t)} \right] \right] \quad (78)$$

In the Schrödinger picture, we have

$$\frac{d\rho}{dt} = -i[H_0, \rho] + e^{-iH_0 t} \frac{d\rho_I}{dt} e^{iH_0 t} \quad (79)$$

Because  $H_0$  commutes with  $\sigma_z^{(j)}$ , we have the expression for the dynamical equation

$$\begin{aligned} \frac{d\overline{\rho(t)}}{dt} &\simeq -i[H_0, \rho] - \lambda'^2 \frac{\tau_c}{2} \sum_{j=1}^n \left[ \hat{\sigma}_z^{(j)}, \left[ \hat{\sigma}_z^{(j)}, \overline{\rho(t)} \right] \right] \\ &= -i[H_0, \rho] + \lambda'^2 \tau_c \sum_{j=1}^n \left( \hat{\sigma}_z^{(j)} \rho \hat{\sigma}_z^{(j)} - \rho \right) \end{aligned} \quad (80)$$

In the low frequency regime where  $\overline{f_j(t') f_{j'}(t'')} = \delta_{j,j'}$ , similarly we have

$$\begin{aligned} \overline{\rho_I(t)} &\simeq \rho(0) - \sum_{j=1}^n \lambda'^2 t^2 \left( \rho(0) - \hat{\sigma}_z^{(j)} \rho(0) \hat{\sigma}_z^{(j)} \right), \\ &= (1 - \lambda'^2) t^2 \rho(0) + \sum_{j=1}^n \lambda'^2 t^2 \hat{\sigma}_z^{(j)} \rho(0) \hat{\sigma}_z^{(j)} \end{aligned} \tag{81}$$

Following similar transformation, we have the expression of the evolution under low frequency noise

$$\begin{aligned} \frac{d\overline{\rho(t)}}{dt} &\simeq -i[H_0, \rho] - \lambda'^2 t \sum_{j=1}^n \left[ \hat{\sigma}_z^{(j)}, \left[ \hat{\sigma}_z^{(j)}, \overline{\rho(t)} \right] \right] \\ &= -i[H_0, \rho] + 2\lambda'^2 t \sum_{j=1}^n \left( \hat{\sigma}_z^{(j)} \rho \hat{\sigma}_z^{(j)} - \rho \right). \end{aligned} \tag{82}$$